Materials Science and Engineering R 40 (2003) 1–46

R Reports: *A Review Journal*

www.elsevier.com/locate/mser

Photovoltaic materials, history, status and outlook

Adolf Goetzberger[a,*], Christopher Hebling[a], Hans-Werner Schock[b]

[a]*Fraunhofer Institute for Solar Energy Systems, Oltmannsstr. 5, D-79100 Freiburg, Germany*

[b]*Institute for Physical Electronics, Universität Stuttgart, Pfaffenwaldring 47, D-70569 Stuttgart, Germany*

Accepted 20 August 2002

Abstract

This paper reviews the history, the present status and possible future developments of photovoltaic (PV) materials for terrestrial applications. After a brief history and introduction of the photovoltaic effect theoretical requirements for the optimal performance of materials for pn-junction solar cells are discussed. Most important are efficiency, long-term stability and, not to be neglected, lowest possible cost. Today the market is dominated by crystalline silicon in its multicrystalline and monocrystalline form. The physical and technical limitations of this material are discussed. Although crystalline silicon is not the optimal material from a solid state physics point of view it dominates the market and will continue to do this for the next 5–10 years. Because of its importance a considerable part of this review deals with materials aspects of crystalline silicon. For reasons of cost only multicrystalline silicon and monocrystalline Czochralski (Cz) crystals are used in practical cells. Light induced instability in this Cz-material has recently been investigated and ways to eliminate this effect have been devised. For future large scale production of crystalline silicon solar cells development of a special solar grade silicon appears necessary. Ribbon growth is a possibility to avoid the costly sawing process. A very vivid R&D area is thin-film crystalline silicon (about 5–30 μm active layer thickness) which would avoid the crystal growing and sawing processes. The problems arising for this material are: assuring adequate light absorption, assuring good crystal quality and purity of the films, and finding a substrate that fulfills all requirements. Three approaches have emerged: high-temperature, low-temperature and transfer technique. Genuine thin-film materials are characterized by a direct band structure which gives them very high light absorption. Therefore, these materials have a thickness of only one micron or less. The oldest such material is amorphous silicon which is the second most important material today. It is mainly used in consumer products but is on the verge to also penetrate the power market. Other strong contenders are chalcogenides like copper indium diselenide (CIS) and cadmium telluride. The interest has expanded from $CuInSe_2$, to $CuGaSe_2$, $CuInS_2$ and their multinary alloys $Cu(In,Ga)(S,Se)_2$. The two deposition techniques are either separate deposition of the components followed by annealing on one hand or coevaporation. Laboratory efficiencies for small area devices are approaching 19% and large area modules have reached 12%. Pilot production of CIS-modules has started in the US and Germany. Cadmium telluride solar cells also offer great promise. They have only slightly lower efficiency and are also at the start of production. In the future other materials and concepts can be expected to come into play. Some of these are: dye sensitized cells, organic solar cells and various concentrating systems including III/V-tandem cells. Theoretical materials that have not yet been realized are Auger generation material and intermediate metallic band material.

Keywords: Solar cells; Crystalline silicon; Thin-film solar cell materials; Amorphous silicon; Chalkogenide solar cells; Organic solar cells

* Corresponding author. Present address: Fraunhofer Inst. f. Solare Energiesysteme ISE, Heidenhofstraβe 2, 79110 Freiburg, Germany. Tel.: +49-761-4588-5152; fax: +49-761-4588-9152.
E-mail address: goetzb@ise.fhg.de (A. Goetzberger).

0927-796X/02/$ – see front matter
PII: S0927-796X(02)00092-X

1. Introduction

1.1. Photovoltaic effect and principle of solar cell operation

One important way to convert solar radiation into electricity occurs by the photovoltaic effect which was first observed by Becquerel [1]. It is quite generally defined as the emergence of an electric voltage between two electrodes attached to a solid or liquid system upon shining light onto this system. Practically all photovoltaic devices incorporate a pn-junction in a semiconductor across which the photovoltage is developed. These devices are also known as solar cells. A cross-section through a typical solar cell is shown in Fig. 1. The semiconductor material has to be able to absorb a large part of the solar spectrum. Dependent on the absorption properties of the material the light is absorbed in a region more or less close to the surface. When light quanta are absorbed, electron hole pairs are generated and if their recombination is prevented they can reach the junction where they are separated by an electric field. Even for weakly absorbing semiconductors like silicon most carriers are generated near the surface. This leads to the typical solar cell structure of Fig. 1: the pn-junction which separates the emitter and base layer is very close to the surface in order to have a high collection probability for free carriers. The thin emitter layer above the junction has a relatively high resistance which requires a well designed contact grid also shown in the figure. The operating principles have been described in many publications [2,3], and will not be addressed further here.

For practical use solar cells are packaged into modules containing either a number of crystalline Si cells connected in series or a layer of thin-film material which is also internally series connected. The module serves two purposes, it protects the solar cells from the ambient and it delivers a higher voltage than a single cell which develops only a voltage of less than 1 V.

1.2. PV world market, market shares of different materials, future prospects

Today's photovoltaic market is about 277 MW (in 2000) corresponding to a value of over US$ 1 billion. This is a remarkable market but still far away from constituting a noticeable contribution to the world energy consumption. Market growth in the last decade was between 15 and 25% as is shown in Fig. 2. This market growth would be very satisfying for any conventional product but in the

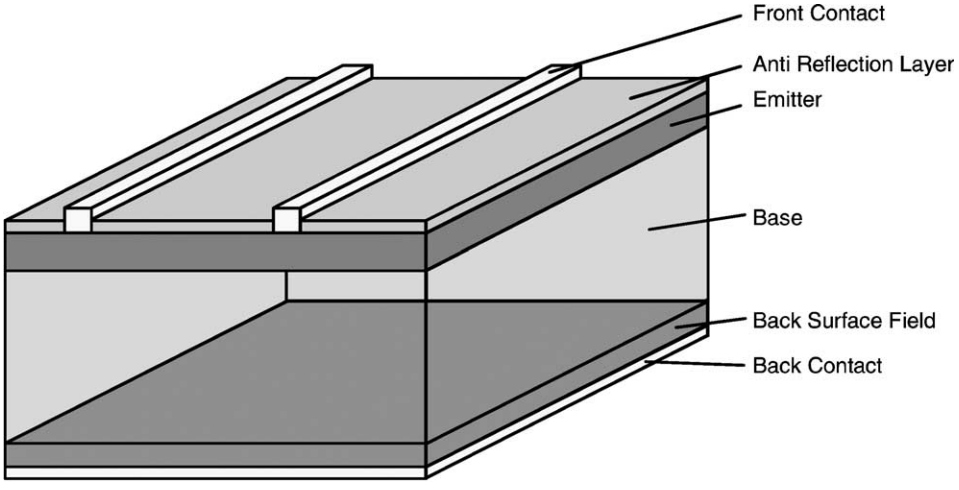

Fig. 1. Typical solar cell.

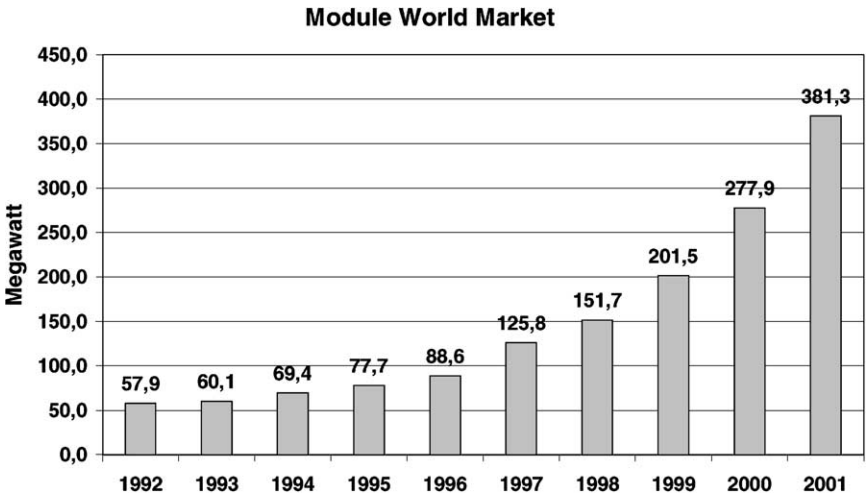

Fig. 2. Development of the world market shares in photovoltaics over the last decade in megawatts per year.

case of PV it is entirely insufficient if we consider the goals. The main motivation for developing solar energy is the desire to get away from depletable fossil fuels with their adverse effect on the environment. At the present growth rate, it will take us far into the second half of this century get a relevant contribution by PV to world energy demand. As will be pointed out below, support programs in several countries are already accelerating market growth. Besides the terrestrial market there is also the space market which has entirely different boundary conditions and also different materials requirements. In order to keep the volume of this paper at a reasonable size, space solar cell materials will not be included.

There are two major market sectors, grid connected and so called stand alone systems. The former delivers power directly to the grid. For this purpose the dc current from the solar modules is converted into ac by an inverter. The latter supplies power to decentralized systems and small scale consumer products. A major market currently being developed is in solar home systems supplying basic electricity demand of rural population in developing countries. The magnitude of this task can be appreciated if one is aware that about 2 billion persons are without access to electricity today. At present, both markets need subsidies, the grid connected installations because PV is much more costly than grid electricity, and solar home systems because the potential users lack the investment capital. On the other hand, there is also a significant industrial stand alone market which is today fully economical.

Because of its high potential the market is hotly contested and new companies are entering constantly. It is significant that several large oil companies have now established firm footholds in photovoltaics. Indeed, a recent study of possible future energy scenarios up to the year 2060 that was published by the Shell company predicts a multigigawatt energy production by renewable energies including photovoltaics [4]. On the other hand, the strong competition leads to very low profit margins of most participants of this market.

In 2000, the market showed an accelerated growth of more than 30%. There are good chances that this growth will continue for at least some years because some countries have adopted aggressive measures to stimulate the grid connected market. Japan's very ambitious 70,000 roof program caused an astonishing increase by 63% of Japanese production in 1999. In Germany, a feed-back law was passed which sets a rebate rate of € 0.5/kWh of PV generated electricity. If this rate is combined with the already existing 100,000 roof program, PV becomes (only moderately) economical. It can be expected that other countries will follow these examples. In order to meet the growing demand, many

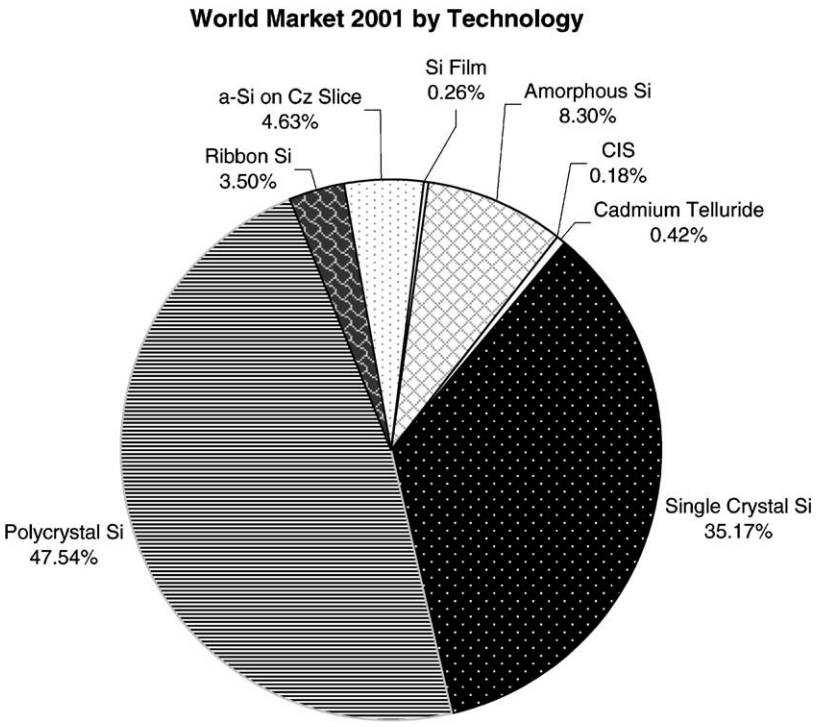

Fig. 3. Market shares of different photovoltaic materials.

PV companies are in the process of setting up substantial new cell and module production capacities. The consequences this will have regarding the availability of semiconductor grade silicon will be discussed in Section 2.5.3.

In spite of the complicated manufacture and the high cost, crystalline silicon still dominates the market today and probably will continue to do so in the immediate future. This is mostly due to the fact that there is an abundant supply of silicon as a raw material, high efficiencies are feasible, the ecological impact is low and silicon in its crystalline form has practically no degradation. The market shares of different technologies in 1999 are shown in Fig. 3. The various forms of crystalline silicon have together a share of 87.6%. Single crystal and cast polymaterial had about equal share for a long time. Recently cast material has surpassed single crystals. Newer types of crystalline silicon like Ribbon and Si-film are not yet very important. A newcomer is a-Si on crystalline silicon (see Section 6). The figure for this material is maybe exaggerated because Sanyo has announced only the beginning of pilot production. Of the true thin-film materials which are summarized as ''others'' amorphous silicon is dominant. As mentioned before, its market it mainly in consumer products. These market shares are rather stable and change only in an evolutionary manner. The dominance of the element silicon in its crystalline and amorphous form is an overwhelming 99%. Of all the other materials only CdTe has a market share but this is less than 1%.

1.3. Requirements for solar cell materials from the point of semiconductor physics for pn-junction solar cells

A large part of the paper will be concerned with silicon although from solid state physics we know that silicon is not the ideal material for photovoltaic conversion. The solar spectrum can be

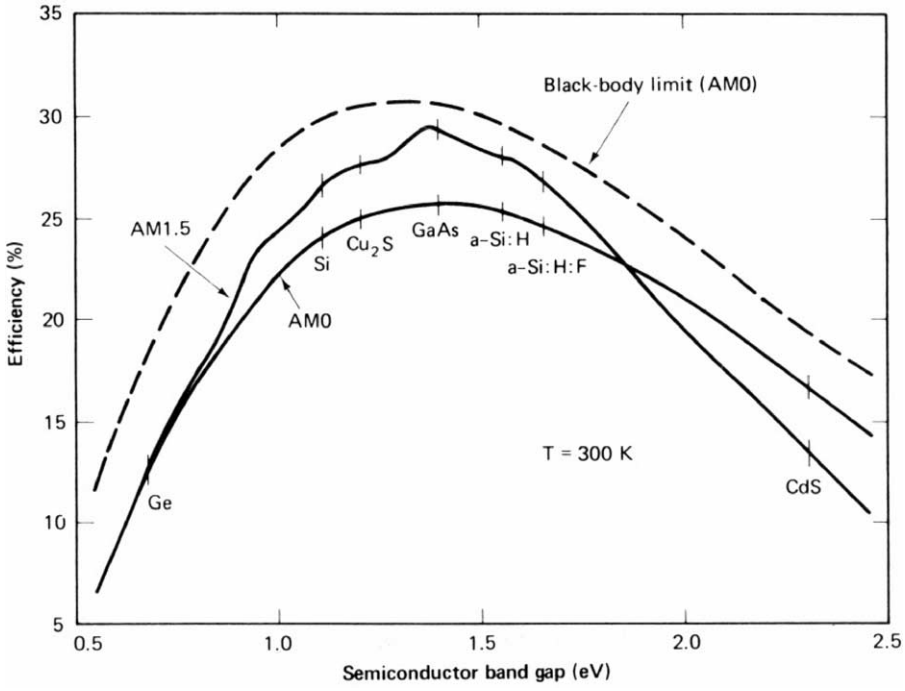

Fig. 4. Dependency of the conversion efficiency on the semiconductor bandgap.

approximated by a black body of 5900 K which results in a very broad spectrum ranging from the ultraviolet to the near infrared. A semiconductor, on the other hand can only convert photons with the energy of the bandgap with good efficiency. Photons with lower energy are not absorbed and those with higher energy are reduced to gap energy by thermalization of the photogenerated carriers. Therefore, the curve of efficiency versus bandgap goes through a maximum (Fig. 4). It can be seen that silicon is not at the maximum but relatively close to it. A much more serious point is that silicon is an indirect semiconductor, meaning that valence band maximum and conduction band minimum are not opposite to each other in *k*-space. Light absorption is much weaker in an indirect semiconductor than in a direct semiconductor. This has serious consequences from a materials point of view: for a 90% light absorption it takes only 1 μm of GaAs (a direct semiconductor) versus 100 μm of Si. The photogenerated carriers have to reach the pn-junction which is near the front surface. The diffusion length of minority carriers has to be 200 μm or at least twice the silicon thickness. Thus, the material has to be of very high purity and of high crystalline perfection. In view of these physical limitations it is quite surprising that silicon has played such a dominant role in the market. The main reason is that silicon technology has already been highly developed before the advent of photovoltaics and high quality material is being produced in large quantities for the microelectronics market.

It is not surprising that a lot of effort has been going and is still going into the search for new materials. Requirements for the ideal solar cell material are:

- bandgap between 1.1 and 1.7 eV;
- direct band structure;
- consisting of readily available, non-toxic materials;
- easy, reproducible deposition technique, suitable for large area production;

- good photovoltaic conversion efficiency;
- long-term stability.

A material fulfilling all these requirements has not yet been found. Since the most important requirement is a high light absorption coefficient the materials defined above are ''thin-film materials'' in the sense that only about 1 μm of active material is required. Thus, the amount of material needed is drastically reduced compared to crystalline silicon. An additional advantage of thin-film materials is that they can easily be connected in series in an integral manner on a large area substrate.

For the future of solar energy materials three scenarios can be envisioned:

- continued dominance of the present single crystal or cast polycrystal technology;
- new crystalline film Si materials of medium thickness either as ribbons or on foreign substrates;
- breakthrough to mass production of true thin-film materials like a-Si or CIS or CdTe.

In the long-term new concepts or new classes of materials like organic solar or III/V-tandem cells also are a possibility. They will be addressed towards the end of this paper.

At this point those scenarios have about equal probability. Even more likely is that two or three of them will coexist for a considerable period and that each technology will find its own market. From an overall point of view it can be considered an advantage that so many avenues exist that potentially lead to a low cost solar cell. In this way the likelihood of achieving this goal is greatly increased.

2. Monocrystalline and multicrystalline silicon

2.1. History

The first silicon solar cell was developed at Bell Laboratories in 1954 by Chapin et al. [5]. It already had an efficiency of 6% which was rapidly increased to 10%. The main application for many years was in space vehicle power supplies. Solar cell technology benefited greatly from the high standard of silicon technology developed originally for transistors and later for integrated circuits. This applied also to the quality and availability of single crystal silicon of high perfection. In the first years only Czochralski (Cz) grown single crystals were used for solar cells. This material still plays an important role. Fig. 5 shows the principle of this growth technique. Polycrystalline material in the form of fragments obtained from highly purified polysilicon is placed in a quartz crucible which itself is located in a graphite crucible and melted under inert gases by induction heating. A seed crystal is immersed and slowly withdrawn under rotation. At each dipping of the seed crystal into the melt, dislocations are generated in the seed crystal even if it was dislocation free before. To obtain a dislocation free state, a slim crystal neck of about 3 mm diameter must be grown with a growth velocity of several millimeters per minute. The dislocation free state is rather stable and large crystal diameters can be grown despite the high cooling strains in large crystals.

2.2. Technology of Czochralski and float zone silicon

Today crystals with diameters of 30 cm and more are grown routinely for the semiconductor market. For solar cells smaller diameter crystals are grown because the usual solar cell dimensions

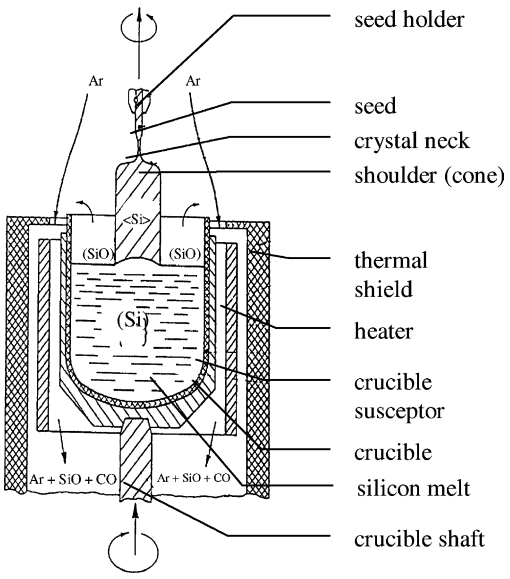

Fig. 5. Principle of the Cz growth technique.

are 10 cm × 10 cm. The round crystals are usually shaped into squares with rounded corners in order to obtain a better usage of the module area.

The silicon melt reacts with every material to a large extent. Only silica can be used as a crucible material, because its product of reaction, silicon monoxide, evaporates easily from the melt. Nevertheless, Czochralski grown crystals contain 10^{17}–10^{18} cm^3 of mainly interstitial oxygen. This leads to lifetime degradation effects described in Section 2.3.

An alternative crystal growth technique is the float zone technique (Fig. 6). A rod of solid, highly purified but polycrystalline silicon is melted by induction heating and a single crystal is pulled from this molten zone. This material is of exceptional purity because no crucible is needed but is more costly than Czochralski (Cz) material. In particular, it has a very low oxygen contamination which cannot be avoided with the Cz-material because of the quartz crucible. Float zone (Fz) material is frequently used in R&D work. Record efficiency solar cells have been manufactured with float zone material but it is too expensive for regular solar cell production, where cost is of overriding importance.

Recently, interesting results have been obtained with an advanced technique, magnetically grown Czochralski (MCz) silicon by Shin-Etsu Handotai in Japan. The principle has been described earlier in [6]. The magnetic field interacts with the free electrons of the silicon and retards convective melt flows. The transport of oxygen from the crucible walls is minimized. Furthermore the distribution of impurities is more uniform.

An interesting new development concerns tricrystals [7]. These are round crystals consisting of three single crystals arranged like pieces of a pie. They can be grown much faster and have higher mechanical stability. Solar cells of 0.1 mm thickness can be manufactured with a saving of 40% of the material.

For solar cells, as well as for all other devices the crystal rods are separated into wafers of 0.2–0.5 mm thickness by sawing. This is a costly process because silicon is a very hard material which can only be cut with diamond plated sawing blades. The standard process was the inner diameter (i.d.) saw where diamond particles are imbedded around a hole in the saw blade. A further disadvantage of this process is that up to 50% of the material is lost in the sawing process. Especially for solar cell wafers a new process was developed, the multiwire saw (Fig. 7). A wire of several

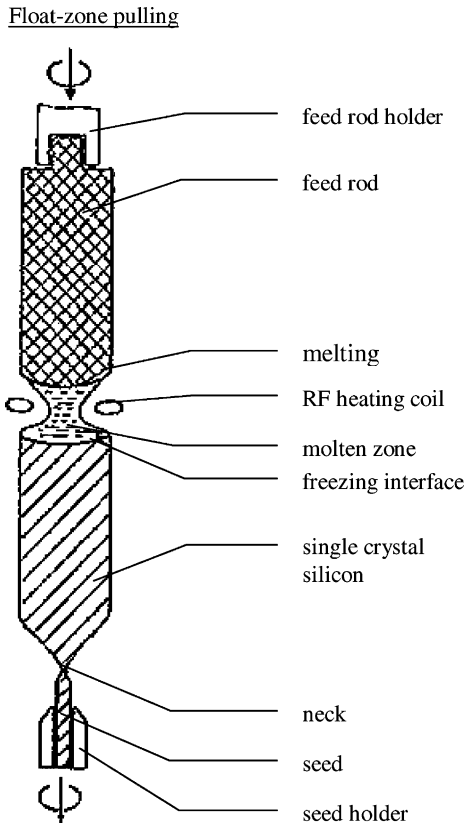

Fig. 6. Principle of the float zone technique.

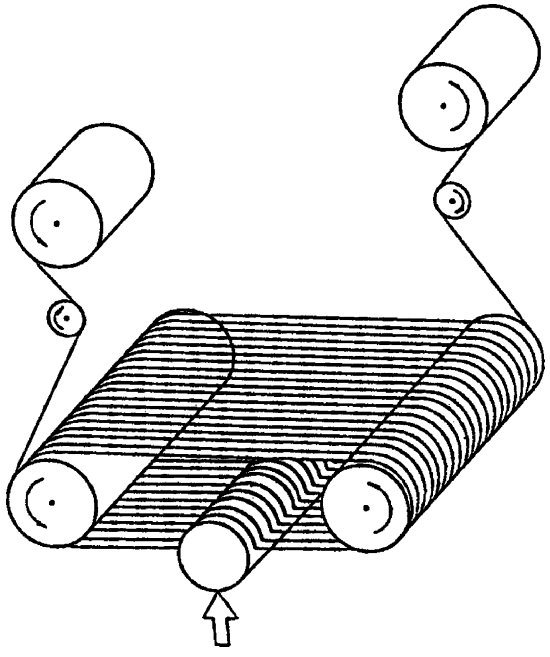

Fig. 7. Multiwire sawing process.

kilometers in length is moved across the crystal in an abrasive suspension, whilst being wound from one coil to another. In this manner, thinner wafers can be produced and sawing losses are reduced by about 30%. It is interesting to note that wire saws are now also used for other silicon devices, an example of synergy in this field.

2.3. Recent results on light induced degradation of minority carrier lifetimes in Cz silicon and practical solutions

2.3.1. The effect and its significance

For many years, it has been known that high efficiency solar cells made from Cz silicon undergo a moderate degradation of efficiency when exposed to light [8]. The efficiency of a cell made from 1 Ω cm silicon degrades from 20.1 to 18.7% within 10 h upon exposure to light [9–12]. This effect, the origin of which remained mysterious for a long time, becomes only now important as solar cells in production reach efficiencies above 15%. It was known that FZ material does not show this behavior but for economic reasons only Cz crystals are used in production. Recently, the reasons for this degradation have been elucidated and ways have been found to prevent it [13]. Because it is a good example of materials research, it will be recapitulated here.

The suppression of the Cz-specific lifetime degradation can easily lead to an absolute efficiency improvement of several percent. This Cz-Si specific lifetime degradation is induced by carrier injection or illumination. After an illumination of about 12 h AM1.5 (depending on the doping level), the lifetime is reduced exponentially to a (fortunately) stable end value. This lifetime degradation can be completely reversed by an anneal step of around 200 °C in room ambient. This phenomenon is very similar to the Staebler–Wronski effect in amorphous solar cells (see Section 5.1).

Observations described in literature [9,10,12,14,15] and obtained within a recent joint research on the light degradation of Cz-Si [16] have drawn a quite complete picture of the symptoms of the metastable defect:

- Boron-doped p-type FZ silicon free of interstitial oxygen and other contamination shows no lifetime degradation.
- Boron-doped p-type FZ silicon intentionally contaminated with oxygen ($\rho_{base} = 6.3\ \Omega\,cm$, $[O_i] = 5.4 \times 10^{17}\ cm^{-3}$) shows a degradation behavior very similar to the one observed in boron-doped p-type Cz-silicon, although no other contaminations are present in these FZ wafers.
- Phosphorus-doped n-type FZ silicon intentionally contaminated with oxygen ($[O_i] = 4.2 \times 10^{17}\ cm^{-3}$) as in (2) shows no lifetime degradation [12].
- Phosphorus-doped n-type Cz silicon shows no degradation [10,11].
- Oxygen-free boron-doped p-type MCz silicon shows no degradation [15].
- G-doped oxygen-contaminated Cz silicon shows no degradation [11].

These observations justify the hypothesis that boron and oxygen are the major components of the metastable defect underlying the Cz-specific lifetime degradation.

In order to investigate the correlation between the defect concentration and the boron and oxygen concentration more than 30 different Cz silicon types from different manufactures and with different oxygen and boron concentrations were analyzed [15]. The electrically active defect concentration was determined using the extent of lifetime degradation by measuring the initial bulk lifetime, τ_0, after a 200 °C anneal step and the final degraded lifetime, τ_d, after an illumination of AM1.5 for at least 30 h. The normalized defect concentration vs. boron concentration with nearly the same interstitial oxygen content is given in Fig. 8. Fig. 9 shows the influence of the interstitial

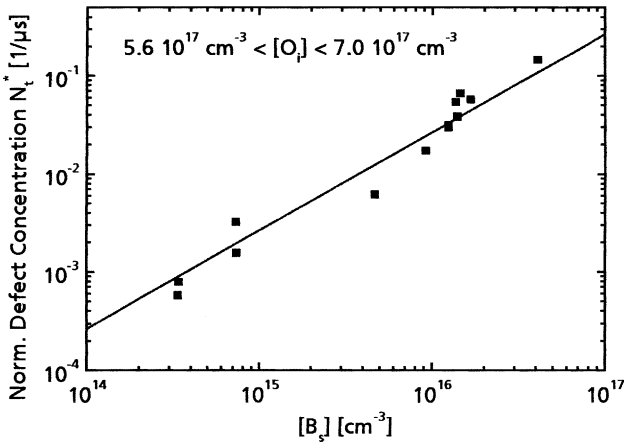

Fig. 8. Normalized defect concentration vs. boron concentration in Cz samples.

oxygen concentration for samples within the same resistivity range. While the defect concentration is increased approximately linearly with the boron concentration, an increasing oxygen concentration increases the defect concentration much stronger (the solid line in Fig. 9 follows an exponential law of power 5).

2.3.2. *Electrical properties of the defect*

The exact physical nature of the defect is not yet known but significant knowledge about its electrical properties has been accumulated. Schmidt et al. [11] have suggested a model assigning the origin of the metastable defect to a B_iO_i complex. The B_iO_i defect was observed by Kimerling et al. [17] in electron-irradiated Cz-Si. Their DLTS measurements showed a DLTS-peak identified as the B_iO_i defect at $E_c - E_t = 0.26$ eV. A recent result points to a different complex of boron with oxygen. From quasi-static injection dependent lifetime measurements an energy level in the range of E_v +0.35 eV to E_c −0.45 eV was inferred [14] for the defect in its active state, which excludes the B_iO_i pair defect. In addition, the fact that a superlinear dependence of the defect concentration on $[O_i]$ is observed (see Fig. 9) supports an unequal contribution of boron and oxygen to the complex

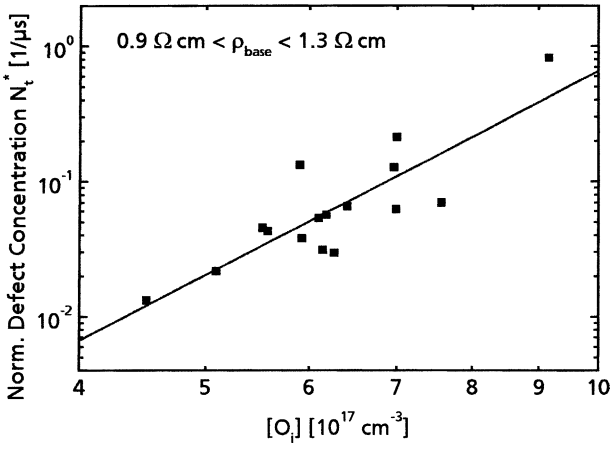

Fig. 9. Normalized defect concentration versus interstitial oxygen concentration for boron-doped Cz samples.

formation. Because of the high recombination efficiency of the state it follows that it has a very large capture cross-section. The energy level of the defect in its passive state was also recently determined by temperature dependent lifetime measurements [18]. It is at 0.08 ± 0.003 eV below the conduction band. This level agrees very well with that of the thermal donor which is well known from the literature and is associated with oxygen in silicon but no definite assignment has been made so far.

2.3.3. Strategies for the reduction or elimination of lifetime degradation

Although the exact nature of the defect is not yet known, effective means of reducing or eliminating the degradation effect have been found. In principle three different ways for the reduction of lifetime degradation can be distinguished.

2.3.3.1. Usage of material with very low concentration or free of oxygen, such as MCz-Si or FZ-Si. The usage of expensive FZ-Si is only feasible for high-efficiency cells. In a recent study [15,16], magnetic Cz (MCz) was used for lifetime studies and solar cell processing. No degradation and excellent lifetimes in the ms-range and efficiencies up to 22.7% were observed [16]. Zhao et al. have processed record cells with an efficiency of 24.5% [19], a value only slightly below the silicon overall record of 24.7% achieved on FZ.

2.3.3.2. Usage of n-type Cz-Si. In principle, it is possible to use n-type Cz-Si but this would entail complete change of the present solar cell technology.

2.3.3.3. Substitution of boron by gallium in p-type Cz-Si. This approach has been pursued in a recent activity [15,16,20] on material grown by Shin-Etsu. Lifetimes above 1 ms before and after a high-temperature process were determined on high-resistivity material (5.2 Ω cm) with a high interstitial oxygen concentration (13.7 ppma). Even if the doping concentration was significantly higher (0.77 Ω cm) the lifetime was excellent (700 μs). Since for all investigated material types no degradation was observed, this approach seems to be very promising. The only disadvantage is the low segregation coefficient of gallium in silicon, resulting in a higher resistivity variation over the crystal length compared to boron doping. The maximum solar cell performance with confirmed efficiencies of 22.5% ($V_{oc} = 689.8$ mV) was achieved on 5.2 Ω cm material [15]. Additionally to these 4 cm^2 cells, 10 cm × 10 cm cells on Ga-doped material with confirmed efficiencies up to 20.2% [21] were produced. This is the highest efficiency achieved on Cz-Si on such a large cell area up to now.

2.3.3.4. Reduction of lifetime degradation by optimized processing. In addition to a proper material choice a reduction of the metastable defect concentration during the cell process should be discussed. Recently, the thermal oxidation process necessary for masking oxides and passivation layers was studied comprehensively by experimental design methods. The ramp-up, oxidation and ramp-down parameters were varied and the effect on the carrier lifetime was studied on different Cz-materials with different interstitial oxygen and boron concentrations. It was possible to distinguish between two principal effects. If the ramping conditions were chosen in a wrong way the bulk lifetime was reduced strongly independently of the plateau conditions. If the ramping conditions were chosen properly an increase of the stable bulk lifetime and a reduction of the extent of degradation, respectively, was observed. For properly chosen ramping parameters, an improvement was obtained within the whole oxidation parameter range, but best results were obtained for temperatures above 1000 °C. The initial lifetime before the process of 12.7 μs can be either decreased down to 0.8 μs (6.3% of the initial lifetime) or increased up to 54 μs (425% of the initial lifetime). Speaking in terms of efficiencies that means a decrease from 18.7 down to 14.9% or an increase up to 20.3%!

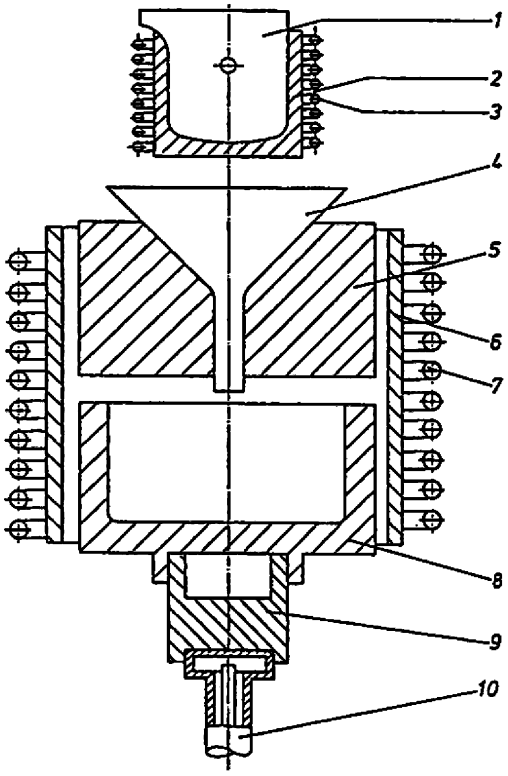

Fig. 10. Crucible for block casting of multicrystalline silicon. The most important numbers in the figure are: 1, premelting crucible; 2 and 7, induction heaters; 4, funnel; 8, crystallization crucible.

In a recent study, a new anneal step at medium temperatures (750 °C) for a short time (10 min) which has the same effectiveness as the higher temperature step mentioned above was demonstrated [18]. This technique is also applicable to rapid thermal processing (RTP) [20].

2.4. Multicrystalline cast silicon

As the cost of silicon is a significant proportion of the cost of a solar cell, great efforts have been made to reduce these costs. One technology which dates back to the seventies is block casting [22] which avoids the costly pulling process. Silicon is melted and poured into a square SiO/SiN-coated graphite crucible (Fig. 10). Controlled cooling produces a polycrystalline silicon block with a large crystal grain structure (Fig. 11).

The grain size is some mm to cm and the silicon blocks are sawn into wafers by wire sawing as previously mentioned. Cast silicon also called polycrystal silicon is only used for solar cells and not for any other semiconductor devices. It is cheaper than single crystal material but yields solar cells with a somewhat lower efficiency. An advantage is that the blocks can be manufactured easily into square solar cells in contrast to pulled crystals which are round. It is much easier to assemble multicrystalline wafers into modules with nearly complete utilization of the module area. Thus, the lower efficiency of cast material tends to disappear at the module level. Because of the contact with the crucible polycrystal silicon has a higher impurity content and, thus, lower carrier lifetime and lower efficiency than monocrystalline silicon. Point defects and grain

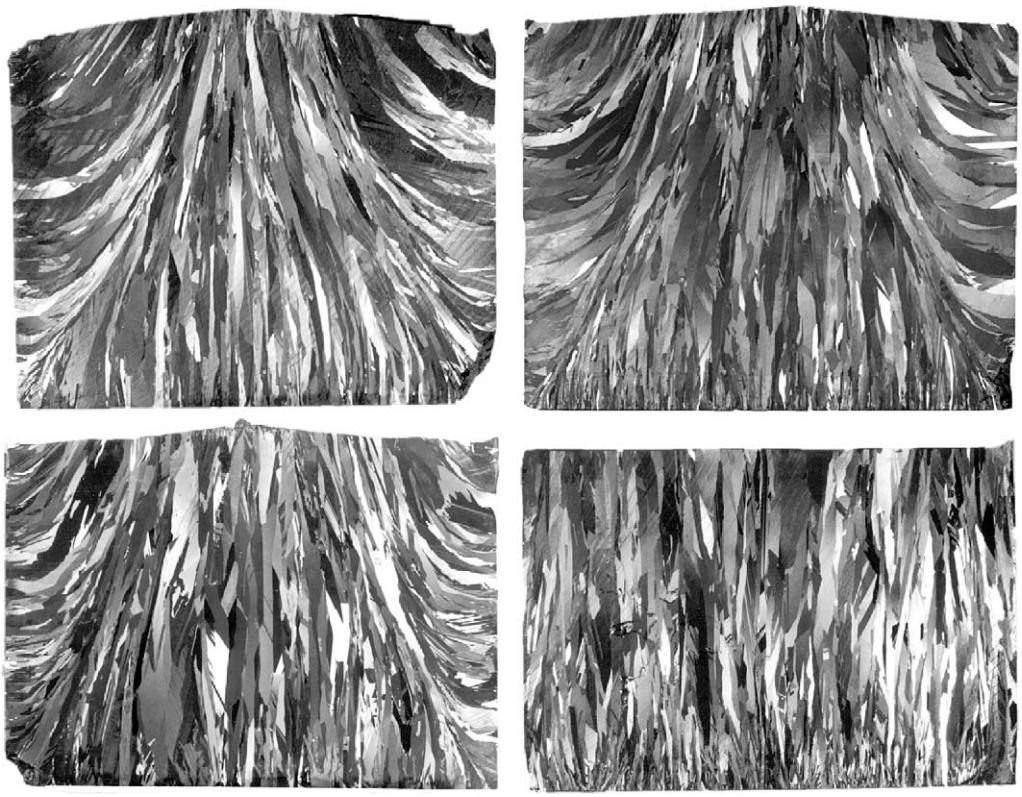

Fig. 11. Cross-sections of multicrystalline Si-blocks which were cooled down under different conditions.

boundaries act in the same direction. Several techniques have been devised to remove impurities during solar cell processing. Mobile impurities can be pulled to the surface by phosphorus gettering [23] which occurs during emitter diffusion. Immobile point defects are deactivated by hydrogen passivation. Atomic hydrogen can diffuse into silicon even at relatively low-temperatures. Processed wafers are exposed to atomic hydrogen produced in a plasma discharge.

2.5. Future prospects in solar cell processing based on crystalline silicon

2.5.1. Status today

Today's photovoltaic market is characterized by the following trends:

- slow but steady improvement of conversion efficiency;
- slow reduction of the cost of modules and systems;
- uncertain supply base of polycrystalline raw material.

In this context, the importance of conversion efficiency has to be discussed. It could be argued that efficiency is not that important, provided the cells are very cheap but reality has demonstrated that solar cells should have a minimum efficiency of about 10% in order to be useful (except for application in consumer products). This has to do with area related cost which constitutes a large part of systems cost. The solar cells have to be hermetically encapsulated in modules which are held in support structures and require electric wiring. All these factors depend on area and have strong influence on the cost of photovoltaic electricity. Therefore, both in research laboratories and

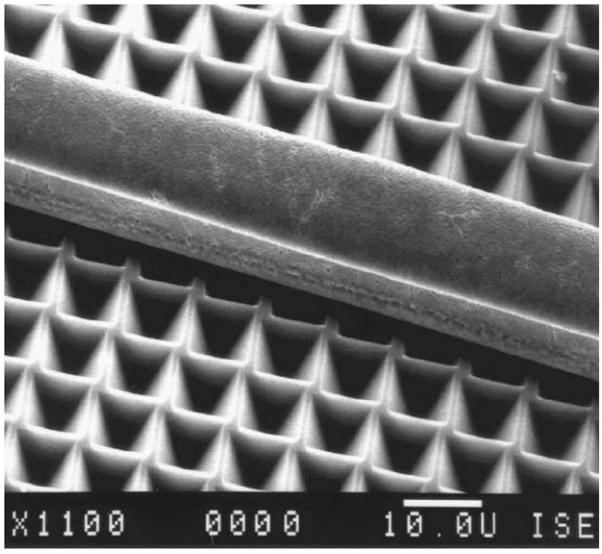

Fig. 12. Inverted pyramids created by isotropic etching.

in manufacturing, improvement of efficiency is a high priority. The best laboratory efficiency for single crystal silicon is today 24.5% [24]. This efficiency can only be realized with very elaborate technology. Experience has shown that progress in laboratory efficiency leads to improvement in production with a certain time delay. The best production cells now have an efficiency of 15–16%.

2.5.2. Texturing

An important aspect related to the choice of material is surface texturization. As the refractive index of Si is very high, reflection at the surface of solar cells has to be minimized. Consequently, all solar cells manufactured today have an antireflective coating consisting of a transparent film of low refractive index. Even more efficient is surface texturing which not only reduces reflection but also provides oblique coupling of light into the cell (Fig. 15, second illustration). In this manner, the radiation paths are increased and enhanced absorption of infrared radiation results. Conventional wet chemical texturization can only be applied to monocrystalline Si. The (1 0 0) surfaces are treated with an isotropic etch (a hot alkaline solution) which creates inverted pyramids bounded by (1 1 1) planes (Fig. 12). Such texturing cannot be applied to polycrystal material because its surface consists of different crystal orientations. Presently, techniques are being developed to overcome this shortcoming. It has been shown that polycrystalline surfaces can be textured by mechanical microtexturization [25], by reactive ion etching [26,27] by acidic etch [28] or by porous silicon [29].

2.5.3. The silicon supply problem

A big question mark for the future is the source of highly purified silicon for solar cells. The 50% of the cost of a module is due to the cost of processed silicon wafers. The PV industry has in the past used reject material from the semiconductor industry that was available at low cost. This created a dependence that is only viable if both sectors grow at the same rate. An additional problem is that the semiconductor market is characterized by violent cycles of boom and depression superimposed on a relatively steep growth curve. In boom times, the materials supply becomes tight and prices

increase. This happened in 1998 when even reject material was in short supply and some solar cell manufacturers had to buy regular semiconductor grade material at relatively high cost.

One of the keys for cost reduction is to reduce the silicon content of the product. Present lines of approach are reduction of kerf loss by wire sawing and use of thinner wafers. The most advanced production lines use wafers of less than 0.2 mm thickness. Thinner wafers are also desirable because if the right technology is used, efficiency is increased [30].

If the present standard technology is to continue its dominance a dedicated solar grade silicon will have to be developed. Even if only a 15% annual growth rate of the market is assumed, there will be a shortage of 5000 Mt by 2010 which is 2/3 of demand [31]. Efforts to produce such material have been undertaken in the past but were not successful for two reasons: purity requirements for solar silicon are very high because photogenerated carriers have to be collected over large distances in such solar cells. This demands high carrier lifetimes and, therefore, an extremely low concentration of relevant impurities. This situation is aggravated by the continued development towards higher efficiencies. The second point is that a dedicated solar grade manufacture is only economical with large scale production. The present market would have to grow by about another factor of five in order to justify such manufacture. The Bayer A.G. recently announced plans to set up a large scale 5000 Mt production plant for solar silicon which could become operational within a few years [31]. The process steps are:

- trichlorosilane production from silicon tetrachloride, hydrogen chloride and hydrogen
- Trichlorosilane pre-purification and silicon tetrachloride recycling;
- one step of trichlorosilane and silicotetrachloride recycling to silane and silicon tetrachloride redistribution;
- silane fine purification;
- thermolytic decomposition of silane to solar grade silicon granules in a fluid bed reactor.

2.5.4. Future

The present technology is relatively mature but several studies have shown that it still has a large cost reduction potential. Like for other industrial products, manufacturing cost follows a learning curve which indicates that for every doubling of manufacturing volume cost drops by 20%. With this learning curve of conventional technology it would take a relatively long time to reach a significant contribution of PV to world energy supply. On the other hand, the crystalline technology has proven itself in the past to be a moving target. Amorphous silicon, for instance has not been able to extend its market share. The major new developments required are an evolutionary further development of technology and a source of solar grade silicon as was outlined above.

3. Ribbon silicon

3.1. History

The goal of crystalline ribbon technologies is to reduce cost by eliminating the costly silicon sawing process and at the same time minimizing the amount of silicon due to a reduced layer thickness. Supposing sufficient bulk quality, the resulting ribbons can be used directly as wafers for solar cell processing. If low quality materials like metallurgical grade silicon are used, a subsequent epitaxial growth of a highly pure active silicon layer is mandatory. In this case, the ribbons are used as a mechanical substrate and an electrical conductor to the back electrode.

There have been tremendous activities in the 1980s in the field of silicon ribbon growth for photovoltaic applications which are described in [32–35]. Out of the over 20 different approaches which had been under investigation, there are mainly five which are still under development or are about to be commercialized. They will be described in the following section.

3.2. The main approaches in ribbon silicon production

3.2.1. The edge defined film fed growth process (EFG)

In the EFG process developed by ASE Americas, a self-supporting silicon ribbon is pulled from the melt through a die which determines the shape of the ribbon [36,37]. Today octagonal tubes of 5.3 m in length at a nominal average wall thickness of 280 μm are pulled out of a graphite crucible containing liquid silicon and are subsequently separated by a Nd:YAG laser [38]. The resulting sheets of 10 cm × 10 cm have a somewhat lower material quality than single crystals, and they have a wavy surface. Nevertheless, conversion efficiencies of up to 14.8% were achieved in the production line with an excellent overall yield of over 90% at the moment and 95% expected in the near future. However, the long-term goal of this approach is to manufacture tubes of cylindrical shape with a diameter of 1.2 m and a wall thickness of about 100 μm [39] (Fig. 13). In the meantime, ASE has expanded the annual capacity of the wafer production to over 13 MW and installed an automated 6.5 MW capacity pilot solar cell manufacturing facility [40].

3.2.2. The string ribbon process

The string ribbon process is under development since 1994 at the Evergreen company and the principles are described in [41,42]. In a fairly simple procedure, silicon ribbons of variable thickness

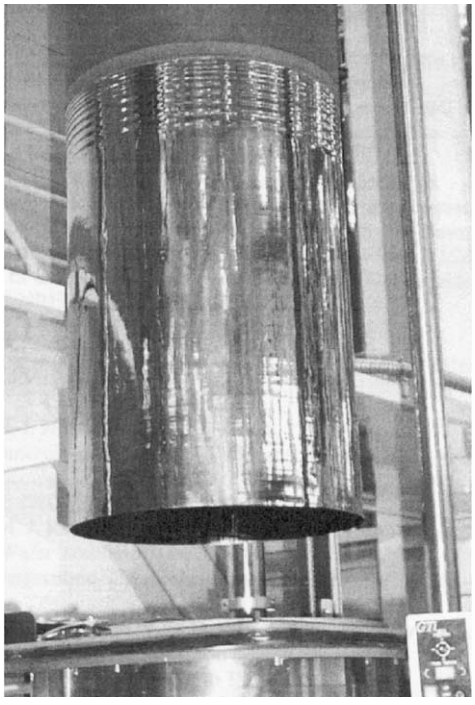

Fig. 13. A 50 cm diameter EFG cylinder grown by ASE Americas [40].

are pulled with two temperature resistant strings directly out of the melt and are cut subsequently into the desired length with diamond tools. The growth speed is up to 25 mm/min resulting in ribbons with a thickness of below 100 μm and a conversion efficiency of 15.1% on a lab cell of 1 cm^2 area [43]. There are 30 and 60 W modules commercially available consisting of cells of 5.6 cm × 15 cm × 0.025 cm size and the production capacity is about to be expanded significantly [44]. The latest development utilizing wraparound contacts for a monolithic interconnection of the cells are described in [45].

3.2.3. Ribbon growth on substrate (RGS)

The main difference of the RGS approach compared to all other processes is that the crystallization direction of the silicon ribbons is not parallel but perpendicular to the pulling direction [46]. The crystallization of the melt is induced by a cooled substrate pulled along the bottom of the crucible. This results in a columnar growth of the grains along the plane normal which enables high pulling speeds and, thus, high production rates [47]. Although efficiencies of up to 11.1% were achieved [48], this material is not commercially available yet.

3.2.4. Silicon sheets from powder (SSP)

The development of the SSP process started in the late 1980s and was considered as a very attractive approach for low cost photovoltaic material [49–51]. The method is originally based on a two-step melting process of silicon powder which is poured onto temporary carrier plates. This results in grains of several mm width and some centimeters length and conversion efficiencies of up to 13% were achieved [34]. In the meanwhile, the activities aiming for SSP material as the active solar cell material were stopped in favor of SSP pre-sheets as substrate material for subsequent deposition of a thin silicon layer. In this process, only a surface melting of the thin silicon powder layer is applied for mechanical reasons followed either by a direct epitaxial growth of a highly pure active silicon layer or by an insulating and protecting SiO_2-intermediate layer. This second approach needs a subsequent recrystallization step since the thin active silicon layer on the SiO_2 layer is very fine-grained after deposition. The advantage of this approach is that very low quality and, thus, very inexpensive silicon like metallurgical grade silicon can be used for the SSP pre-sheet. The latest results achieved with the various silicon materials and recrystallization methods are described in [52] (Fig. 14).

3.2.5. Dendritic web

The dendritic web method, which was first published in 1985, produces single crystalline ribbons in a fairly cost effective process [53]. Although the highest conversion efficiencies on ribbon materials were realized on dendritic web ribbons (17.3%), there is very little known about the technical status and possible plans for its commercialization [54].

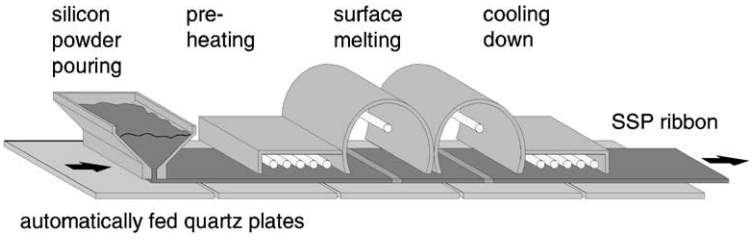

Fig. 14. Silicon sheets from powder (SSP) apparatus developed at Fraunhofer ISE [52].

4. Crystalline thin-film silicon

4.1. History

The first considerations concerning thinner silicon wafers for solar cells were made by Wolf and Lofersky while simulating the ideal parameters for record high efficiencies [55,56]. They pointed out that with decreasing cell thickness, the open circuit voltage increases due to the reduced saturation current which again is a result of a decreasing geometry factor. In these papers, the benefits of a thickness in the order of 30 μm were quantified, also demonstrating the importance of low surface recombination velocities and a good optical confinement to make use of this advantages. The first theoretical work about light trapping in silicon layers was performed by Goetzberger who suggested a Lambertian back reflector as a simple but efficient structure [57]. Different possibilities of light trapping are shown in Fig. 15. The wide range of technological advantages incorporating the potential for a significant cost reduction was also described by Goetzberger et al. [58]. After these fundamental works, it took more than a decade until an increasing number of groups singled out the various technological problems and realized first test solar cells to overcome these problems. Nowadays, the driving force for the development of crystalline silicon thin-film solar cells (c-SiTFC) is the inherent possibility for cost reduction, although this advantage has not yet been converted into commercial products. There are various overview articles describing the ongoing research activities in the different approaches which are recommended for more detailed information [59–64].

An illustration of the conversion efficiencies as a function of the grain size achieved by the different institutes is given in Fig. 16.

4.2. The basic components of a crystalline silicon thin-film solar cell

The linking feature of all c-SiTFC approaches is the underlying substrate needed as a mechanical support due to the reduced thickness of the active silicon layer of typically 5–50 μm. The substrate consists either of low quality silicon like the previously mentioned SSP-ribbons, or of foreign substrates such as glass, ceramics or graphite. The choice of the substrate material determines the maximum allowed temperature for solar cell processing and, therefore, nearly all

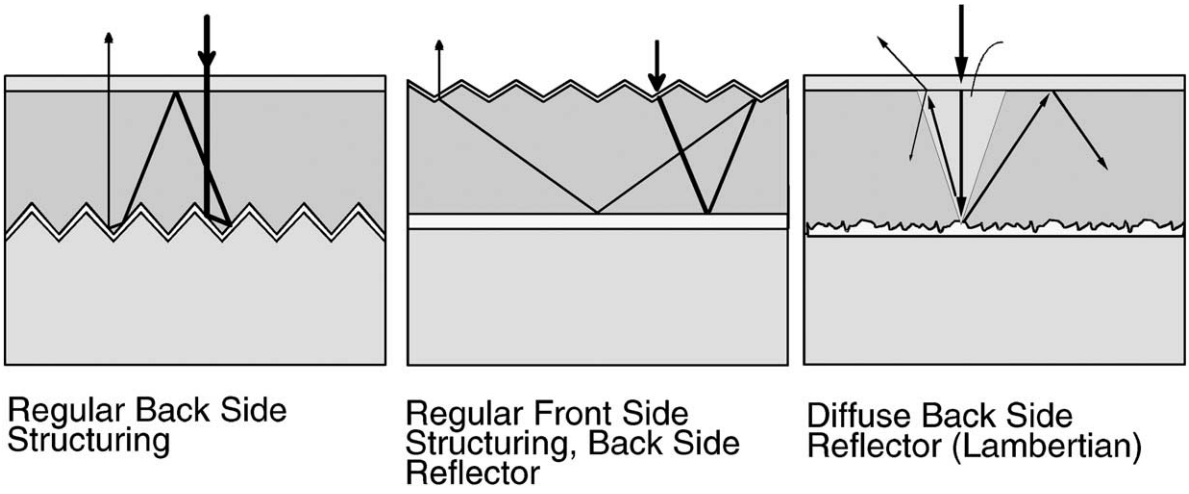

Fig. 15. Optical confinement for light path enhancement.

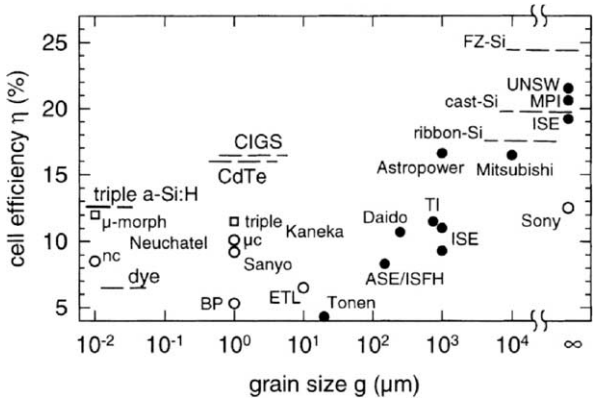

Fig. 16. Realized solar cell efficiencies as a function of the grain size [61].

c-SiTFC approaches can be assigned to one of the three categories: (i) high-temperature approach; (ii) low-temperature approach; and (iii) transfer techniques which are described below. Furthermore, the use of electrically conductive substrate materials enables the conventional front- and backside cell conducting scheme, insulating materials allow for the monolithic series-interconnection of several cells. The most critical requirements concerning the substrate are low cost, thermal stability, a matching thermal expansion coefficient, mechanical stability and a certain surface flatness [59,61] (Fig. 17).

Due to the high temperatures which arise in the cell processing, impurities might migrate from the substrate into the active silicon layer with harmful effects on the conversion efficiency [65]. Therefore, the deposition of barriers layers like SiO_2 or SiN_x on the substrate prior to the deposition of the electrically active silicon layer is an effective measure in order to suppress the impurity diffusion [66]. Furthermore, such intermediate layers can act as a backside reflector in order to achieve a good optical confinement. An excellent overview over the electrical and optical properties of intermediate layers is given in [67].

There is a large variety of silicon deposition technologies which can roughly be allocated to the main groups liquid phase and gaseous phase deposition. In the liquid phase deposition, the respective substrate is brought into contact with a metal melt (Cu, Al, Sn, In) saturated with silicon. By lowering the temperature of the melt supersaturation occurs and silicon is deposited on the substrate. The substrate temperature lies within the range of 800–1000 °C and deposition rates vary from a few

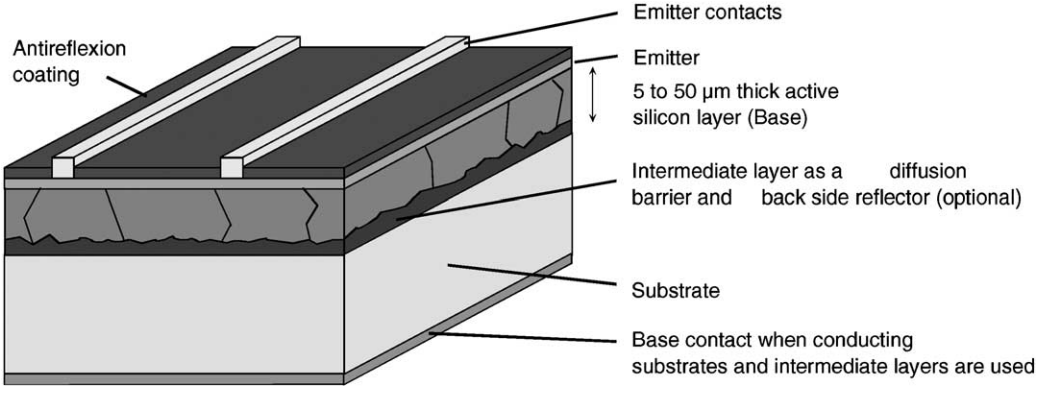

Fig. 17. The basic components of a crystalline silicon solar cell.

micrometers per hour to up to 10 μm/h [68,69]. The term liquid phase epitaxy (LPE) process is also used when the growth is not epitaxial. In the chemical vapor deposition (CVD) method, which is a well-established method in microelectronics, a mixture of H_2 and the precursors SiH_4, SiH_2Cl_2, or $SiHCl_3$ is decomposed thermally at the hot surface of the substrate. The most common techniques are low pressure and atmospheric pressure CVD (LP-CVD, AP-CVD), but also plasma enhanced, ion-assisted or hot-wire CVD (PE- CVD, IA-CVD, or HW-CVD) are used to deposit silicon films at temperatures between 300 and 1200 °C. There is little known about the economical aspects of the different deposition methods when used in large scale production of solar cells, but there is a trend towards APCVD due to the potential for continuous inline processing and realized deposition rates of more than 5 μm/min.

As a general trend, the cell efficiency increases with the grain size. This is due to the fact that grain boundaries in their unpassivated state can be very effective recombination centers which reduce the diffusion length of the minority carriers drastically. On the other hand, it is well known from simulations that the diffusion length should exceed the thickness of the active Si-layer at least two times in order to achieve high conversion efficiencies. Therefore, whenever the Si-films are deposited on intermediate layers or foreign substrates and thus are too fine-grained for acceptable minority carrier mobilities, an upgrading by recrystallization is recommended. Various methods have been used, depending on the procedure used to couple the energy into the Si-layer and depending on the thermal budget which is allowed from the substrate. The most common recrystallization mechanisms which occur via the liquid phase are laser, electron-beam, strip heater or halogen lamp recrystallization. They are distinguished according to the form and size of the liquid zone, the pulling speed of the Si-grains, the melting depth, the three-dimensional temperature gradient and, thus, the grain size and defect density in the resulting Si-layer and finally the scalability of the apparatus (Fig. 18).

Finally, the solar cell technology for Si-thin-film solar cells has to be adopted in several ways:

- Due to the weak absorbance of crystalline Si, the light trapping is one of the crucial measures which have to be applied in order to realize a high degree of total internal reflection. This can be achieved by a Lambertian back side reflector or by a textured front surface in combination with a reflecting back side [57].
- The electrical passivation of the surfaces is important in order to enhance the diffusion length of the charge carriers. This is done for example by an SiO_2-layer on the front side and by a thin highly doped Si-layer forming a back surface field which prevents the charge carriers from recombination at the back side.
- If non-conducting intermediate layers or substrates are used, both the emitter and the base contacts have to be applied on the front side. The emitter contacting can be done conventionally, but the

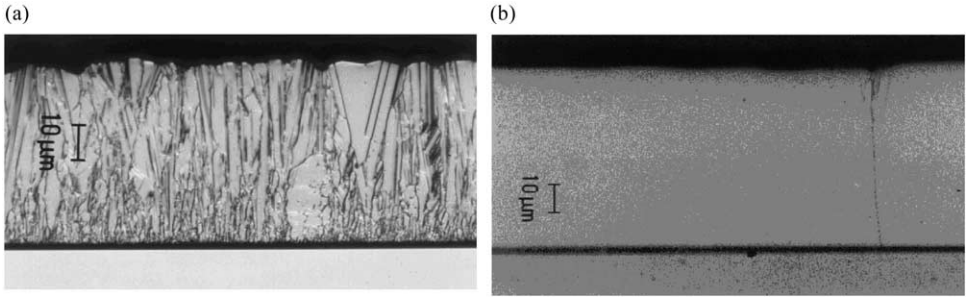

Fig. 18. Si-layer deposited on a SiO_2-intermediate layer (a) and after a zone melting recrystallization step (b).

base must be contacted either by a selective emitter, or by trenches etched through the homogeneous emitter [70]. Such a front contacting scheme enables the possibility of an integrated series-interconnection of several cells resulting in a monolithic solar cell module on a single substrate.

- For the solar cell formation, the layer system is processed with various temperatures due to the silicon deposition, silicon recrystallization, emitter formation, impurity gettering, electrical passivation of the surface or of the bulk silicon, deposition of anti-reflection layers or the deposition of the electrodes. The individual thermal steps as well as the total thermal budget are other crucial parameters for a successful manufacturing of c-Si thin-film solar cells.

4.3. The present status of the crystalline silicon thin-film solar cell

There is a wide range of research activities worldwide that have demonstrated the efficiency potential of thin crystalline silicon with conversion efficiencies of up to 21% under ideal conditions. Mostly, the aim is to prove the respective concept and to study the influence of the most crucial electrical and optical parameters. Generally, it must be noted, that most realized cells were still made on Si-wafers as substrates. Such test structures were made under ideal conditions using the best understood materials available aiming to prove the respective concept and to study the influence of the different boundary conditions on the cell performance. The insights gained from these ideal systems are now about to be transferred into cost-effective layer-systems and processing technologies. Table 1 summarizes the results which have been obtained so far in terms of realized and published silicon thin-film solar cells as well as in terms of silicon ribbon solar cells. It can be seen, that the crystalline Si thin-film solar cell has seen a tremendous development in the last decade although only Astropower transferred this effort into a commercially available product. On the background of the success of the Si-ribbon solar cells, it is still not clear if the various crystalline Si thin-film cells will significantly contribute to the solar cell landscape in the future.

The large number of different approaches can roughly be classified into the three categories: (i) Si-layers directly deposited on glass; (ii) Si-layers on high-temperature resistant substrates; and (iii) semi-processed monocrystalline Si-layers from Si-wafers transferred onto glass. Some outstanding results which were obtained within this classification will be discussed in the following sections.

4.3.1. Si-layers deposited directly onto glass

The inherent limitation of all approaches compatible with glass substrates is the melting point of the glass which is on the order of 600 °C. This means that both the Si-deposition and the solar cell processing is not supposed to go beyond this temperature limit for a longer period of time. The crystallization of the Si-layer can be done either by laser- or by solid-phase crystallization. Kaneka Corp., for example, utilizes a laser crystallization of a highly doped contact layer followed by the deposition of an intrinsic microcrystalline absorber film. The crucial feature of this surface texture and enhanced absorption with a back reflector (STAR)-structure is a Si-layer thickness of less than 5 μm combined with an excellent optical confinement due to a rough reflecting back layer [71]. A triple cell stack of a a-Si:H/μc-Si/μc-Si achieved a stable efficiency of 11.5% (Fig. 19).

The Center for Photovoltaic Devices at the University of New South Wales and the Pacific Solar Corp. are exploring the so-called multijunction solar cell concept applying the deposition of a high number of layers with alternating p- and n-doping level. The basic idea is that very short minority carrier diffusion lengths can be tolerated in these layers and, thus, very impure material can be used. The conversion of this benefit into a good cell performance depends strongly on the electrical connection of the layers with the same polarity and on the recombination in the space charge region.

Table 1
Solar cell results obtained on thin crystalline silicon layers and on silicon ribbon materials[a]

Institute/company	Reference	Substrate	Concept	A (cm^2)	W (μm)	η (%)	V_{oc} (mV)	I_{sc} (mA/cm^2)	FF (%)
ASE/ISFH	[89]	Graphite, SiC	CVD-Si, ZMR, CVD-epi-Si	1.3	30	8.3	561	20.1	73.6
Astropower	[80]	Unknown	Silicon-Film™, proceedings unpublished	1.0	100	16.6	608	33.5	81.5
Astropower	[80]	Unknown	Silicon-Film™, proceedings unpublished	240	100	12.2	581.9	27.4	76.5
Astropower	[80]	Steel	Silicon-Film™, product I	0.1	–	9.6	536	26.0	68.5
Astropower	[90]	Graphite cloth	Silicon-Film™	1	>80	13.4	599	28.4	78.6
Australian National University	[91]	mc-Si, p^+	LPE-Si	4	30	15.4	612	28.0	76.0
Australian National University	[92]	Si-wafer	LPE-Si, substrate thinned	4	28	17.0	651	32.6	80.3
Daido Hoxan Corp.	[79]	Carbon fiber	Plasma sprayed Si, recrystallize	1.0	500	10.7	527.9	31.1	68.5
ETL	[93]	Al_2O_3, Si_3N_4-IL	CVD-Si, laser-ZMR	0.01	4.2	6.5	480.0	25.5	53
ETL	[94]	Al_2O_3, Si_3N_4-IL	Plasma-CVD, electron beam-recrystallize	0.023	2	1.44	0.25	19.2	30.1
Evergreen Solar	[43]	Silicon	String ribbon	1	100	15.2	588.0	33.7	76.1
Fraunhofer ISE	[76]	SIMOX wafer	CVD-epi-Si, p^+/p	4	46	19.2	667.6	37.1	77.7
Fraunhofer ISE	[95]	FZ-Si, p^+	CVD-epi-Si	4	40	17.4	658.1	32.0	82.6
Fraunhofer ISE	[96]	mc-Si, p^+	RTCVD-epi-Si, ZMR	1	13	12.8	589	29.9	74.5
Fraunhofer ISE	[52]	SSP-Si, SiO_2-IL	Large area recrystallization	1	30	11.2	563.7	27.1	75.3
Fraunhofer ISE	[97]	Si-infiltrate SiC	LPCVD-Si, ZMR, CVD-Epi	1	72	9.3	567	21.6	76.1
Fraunhofer ISE	[67]	Si_3N_4, ONO-IL	PECVD-Si, ZMR, CVD-Epi	1	30	9.4	539	26.1	67
ISE/ASE	[70]	Graphite, SiC	CVD-Si, ZMR, CVD-epi-Si	1	30	11.0	570	25.6	75.5
Georgia Tech.	[54]	Dendritic web	Silicon ribbon, monocrystalline	4	100	17.3	618	35.4	79.2
Hitachi	[98]	Corrugated FZ-Si	V-grooves on thinned wafer	–	–	12.3	556	33.5	66
IMEC	[99]	mc-Silso Si, p^+	APCVD-epi-Si, H^+-passivation	4	20	13.9	615	27.5	78.4
IMEC	[100]	RGS-Si	APCVD-epi-Si, H^+-passivation	4	30	10.4	558.0	24.5	75.8
IPE	[86]	FZ-Si, porous	CVD, transfer-technique onto glass	4	24.5	14.0	634.2	27.3	80.5
Kaneka	[71]	Glass	PECVD poly-Si STAR-structure	1	3.5	9.4	480	26.1	74.8
Mitsubishi	[101]	Cz-Si, SiO_2-IL	CVD-Si, ZMR, substrate-etched	4	60	16.5	608	35.1	77.1
Mitsubishi	[102]	Cz-Si, p^+	VEST-structure	96	77	16.0	588.7	35.6	76.3
Mitsubishi	[103]	Cz-Si, SiO_2-IL	CVD-Si, ZMR	100	–	14.2	608	30.0	78.1
MPI-FKF	[104]	Fz-Si, p^+	LPE-Si (In)	1	16.8	14.7	659	27.2	80.2
MPI-FKF	[105]	FZ-Si	Thinned FZ-wafer	1	47	20.6	683	37.4	80.8
MPI-FKF	[60]	Cz-Si, p^+	CVD-epi-Si	4.1	50	17.3	655	32.5	81.1
NREL	[106]	Cz-Si	LPE-Si (Cu/Al), substrate dipping	1	5	15.3	573.1	32.6	81.6
Sanyo	[107]	Metal	Solid phase crystalline (SPC)	1	5.2	9.2	553	25.0	66.4
Sony	[85]	Cz-Si	Epitaxy on porous Si (transfer)	4	6	12.5	623	25.5	79.0
Tonen	[108]	Glassy carbon	DC-RF plasma-sprayed Si	–	–	4.3	426	16.7	64.3
Uni Neuchatel	[109]	Glass	PECVD-Si (micromorph)	0.3	–	12.0	1280	13.5	69.2
UNSW	[73]	FZ-Si	Thinned wafer	4	47	21.5	698.5	37.9	81.1
UNSW	[110]	Cz-Si, p^+	LPE (Ga/In)	4.0	32	16.4	645	32.3	78.5
UNSW	[111]	FZ-Si, p^+	LPE, thinned Si on glass	4	25	15.6	649	29.9	80.2
UNSW	[72]	Cz-Si, p^+	Six layers n–p CVD-epi-Si	4	32	17.6	660.7	32.8	81.4
ZAE	[112]	Fz-Si, porous	IAD, transfer technique onto glass		7	4.4	501	14.6	60.0

[a] ZMR: zone melting recrystallization; CVD: chemical vapor deposition; LPE: liquid phase epitaxy; APCVD: atmospheric pressure CVD; LPCVD: low pressure CVD; RTCVD: rapid thermal CVD; PECVD: plasma enhanced CVD; IL: intermediate layer; IAD: ion assisted deposition.

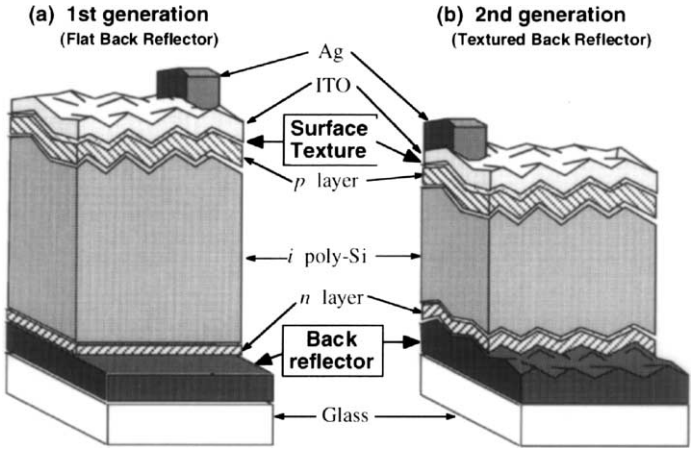

Fig. 19. STAR-Structure developed at Kaneka Corp., Japan.

Efficiencies of up to 17.6% were obtained with a six-layer system deposited epitaxially on a highly doped Cz-wafer in order to proof the concept, but no results are reported on a low cost system. [72,73].

4.3.2. Si-layers on high-temperature resistant substrates

The high-temperature approaches are relying on the high Si-deposition rates (≅5 μm/min) at temperatures beyond 1000 °C and Si-recrystallization techniques via the liquid phase ($T_{melt,Si} \sim 1420$ °C). With these technologies, a high-throughput, a continuous inline-processing, large grains and, thus, high efficiencies can be obtained. On the other hand, a substrate material with ideal technical properties at a low price could not be found yet. As a general rule, inexpensive materials usually contain a high level of impurities which causes the migration of these impurities from the substrates into the active Si-layer at high temperatures. Furthermore, the complexity of the process steps for the layer preparation and the solar cell processing particularly on insulating substrates counts on the critical side.

The Fraunhofer Institute for Solar Energy Systems (ISE) is investigating three different high-temperature approaches:

- Highly doped SSP (see Section 3.2.4) pre-sheets are used as substrates for a subsequent direct epitaxial growth of the active Si-layer in a rapid thermal chemical vapor deposition (RT-CVD) reactor [52,74]. The thermal processing of the layer system for solar cells has to take into account that the impurities migrate into the active Si-layer and, thus, the maximum allowed impurity level in the substrate has to be determined.
- A highly doped Si-sheet of low quality as a substrate which is covered subsequently by a SiO_2-layer with via holes. The total area coverage of the holes is 0.5% which is enough to maintain a sufficient electrical contact to the back electrode but still suppresses the diffusion of impurities from the substrate significantly. The CVD-deposited Si-layer on top is exposed to a large area recrystallization step in order to enlarge the grain size, and the seeding occurs via the Si-crystals which are located underneath the via-holes.
- Encapsulated foreign substrates such as ceramics or graphite are used and the upgrading of the fine-grained Si-layer occurs with a zone melting recrystallization step. An interdigitated front contact scheme was developed for such SOI (Silicon-On-Insulator)-structures which allows the emitter and the base electrode formation at the front side. An efficiency of 11% was realized on an

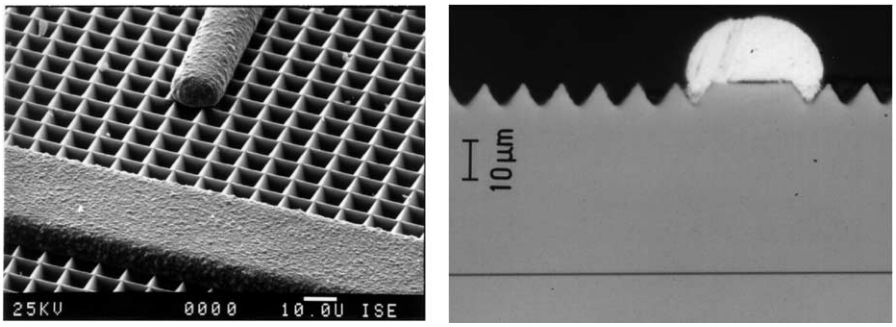

Fig. 20. Epitaxially grown Si-layer of 46 µm thickness on an insulating SiO_2-layer (SIMOX-wafer) processed as a solar cell. Efficiencies of up to 19.2% were achieved with an interdigitated front grid for the emitter and the base contacting.

SiC-covered graphite substrate from ASE [70] as well as 9.4% on silicon nitride [75]. In order to study the potential of such a front-contacted SOI structure (silicon on insulator), epitaxially grown CVD layers on SIMOX-wafers were processed to solar cells which resulted in efficiencies of up to 19.2% (Fig. 20). Additionally, 24 series-connected cells of 1 cm^2 size each on one SIMOX-wafer, using such an interdigitated front grid achieved an open circuit voltage of 15.2 V [76,77].

The approach of Mitsubishi Corp. also relies on their knowledge of the SOI-technology and focuses on the formation of a high quality mc-Si layer on an insulator. A 3 µm thick LPCVD layer deposited on a SiO_2 layer is zone-melted in a strip heater resulting in grains of cm-length and defect densities on the order of some 10^6 cm^{-2}. After the epitaxial growth of the 60 µm thick active Si-layer, the supporting Si-wafer is etched back by a patterned mask for back electrode formation. The 16.45% conversion efficiency is the highest value obtained by means of recrystallized Si-layer [78].

Daido Hoxan Corp. used plasma spraying to deposit Si-films with a thickness of 500 µm and an efficiency of 10.7%. [79]. Deposition rates of up to 10 µm/s can be achieved with this method.

The only thin Si-cell concept which made it to a commercially available product is the Silicon Film™ technology developed by Astropower [80]. Very little is known about this approach, but the active Si-layer is probably deposited on a micro-grooved, conducting ceramic substrate which is covered by an intermediate layer as a back reflector and diffusion barrier. The grains are about 2 mm in diameter and the electrical contact to the back electrode is made by via holes in the dielectric layer. As important process steps, impurity gettering and hydrogen passivation serve to boost the minority carrier diffusion length. A remarkable efficiency of 16.6% was achieved on 1 cm^2 in the laboratory; cells of 15 cm in width and variable length went into production.

4.3.3. Transfer technologies of monocrystalline thin Si-films onto glass

The approaches based on transfer technologies of thin monocrystalline Si-films are the latest and very exciting developments within the crystalline Si thin-film community. The basic idea is to detach a semi-processed thin monocrystalline Si-layer from the FZ-wafer and to transfer it onto a glass substrate. The advantages are obvious: the superior material quality enables very high efficiencies even from less than 40 µm thick Si-layers, inexpensive glass can be used as substrate and finally, the FZ-wafer can be reused for the thin-film formation and detachment for several times. In the meantime some promising results were obtained, but up to now no wafer was used for the layer formation for several times. After some pre-studies with semi-processed FZ-wafers which were

attached via ethylene vinyl acetate (EVA)-foil to a glass substrate and thinned wet-chemically from the back side [81], there are currently five main approaches under development [61].

The first real Si-transfer approach was pursued by R. Brendel with the so-called Ψ-process. A textured (1 0 0)-oriented Si-wafer with a porous Si-film serves as an epitaxial seed for the growth of an approximately 10 μm thick monocrystalline Si-film. The epitaxial growth serves to conformally coat the surface of the anodically etched porous Si, resulting in a waffle-like structure enclosed by (1 1 1) planes [82]. Simulations predicted efficiencies of up to 19% under ideal technological conditions.

The epi-lift process which was developed at the Australian National University (ANU) is based on the formation of (1 1 1)-oriented crystal planes during near-equilibrium growth of Si using liquid phase epitaxy. An oxidized, (1 0 0)-oriented Si-wafer with oxide-free seed lines oriented close to two orthogonal (1 1 0)-directions on the wafer surface serves as a substrate for epitaxial Si-growth by liquid phase epitaxy (LPE). This approach aims at the fabrication of a solar cell from the monocrystalline Si-net and to detach it from the wafer by using a suitable etch [83].

Mitsubishi Electric Corp. developed the so-called via-hole etching for the separation of the thin-film (VEST)-structure where a Si layer is CVD-deposited and recrystallized on a SiO_2-covered mono-Si substrate. After the realization of this SOI-structure, via-holes are etched with 100 μm diameter and 1.5 mm distance to each other. The Si-layer is subsequently detached from the wafer by HF-etching of the SiO_2-intermediate layer through the via-holes. Solar cells were realized with this approach having a thickness of 77 μm, an area of nearly 100 cm^2, and efficiencies of up to 16.0%. This is a remarkable success, especially due to the fact that the back contacts were screen printed on this fragile structure [84].

Sony Corp. pursues the epitaxial growth of monocrystalline Si-film on the thermally annealed crystalline surface on top of a highly porous buried Si-level. The Si-layer for the solar cell can be detached from the wafer due to the mechanically fragile separation layer underneath. Using a 12 μm thick epitaxial film that was transferred on a plastic foil, a conversion efficiency of 12.5% on 4 cm^2 was achieved [85].

The Institute of Physical Electronics also relies on the epitaxial growth of the active Si-layer on a so-called quasi-monocrystalline Si-film. Again, a buried porous layer enables the separation of the solar cell from the wafer and the transfer of the processed cell to a foreign superstrate. Due to an excellent light-trapping scheme, efficiencies of up to 14.0% were obtained with this approach. Furthermore it could be shown, that the starting wafer can be used several times as a seeding wafer for the porous layer formation and the subsequent epi-growth [86] (Fig. 21).

5. Amorphous silicon

5.1. History

The first publications on amorphous silicon (a-Si) relevant for solar cell fabrication appeared after the late 1960s [113–115]. The first paper at a photovoltaic conference was presented in the 12th IEEE PVSC (1976). Only 5 years later, the first consumer products appeared on the market. However, it took quite some time until the basic properties of the material were understood. The history is full of misinterpretations of experimental data, in particular the role of hydrogen in the amorphous network [116]. More than 20 years have already passed since the first solar cell from amorphous silicon has been reported by Carlson in 1976. The high expectancy in this material was curbed by the relatively low efficiency obtained so far and by the initial light induced degradation for

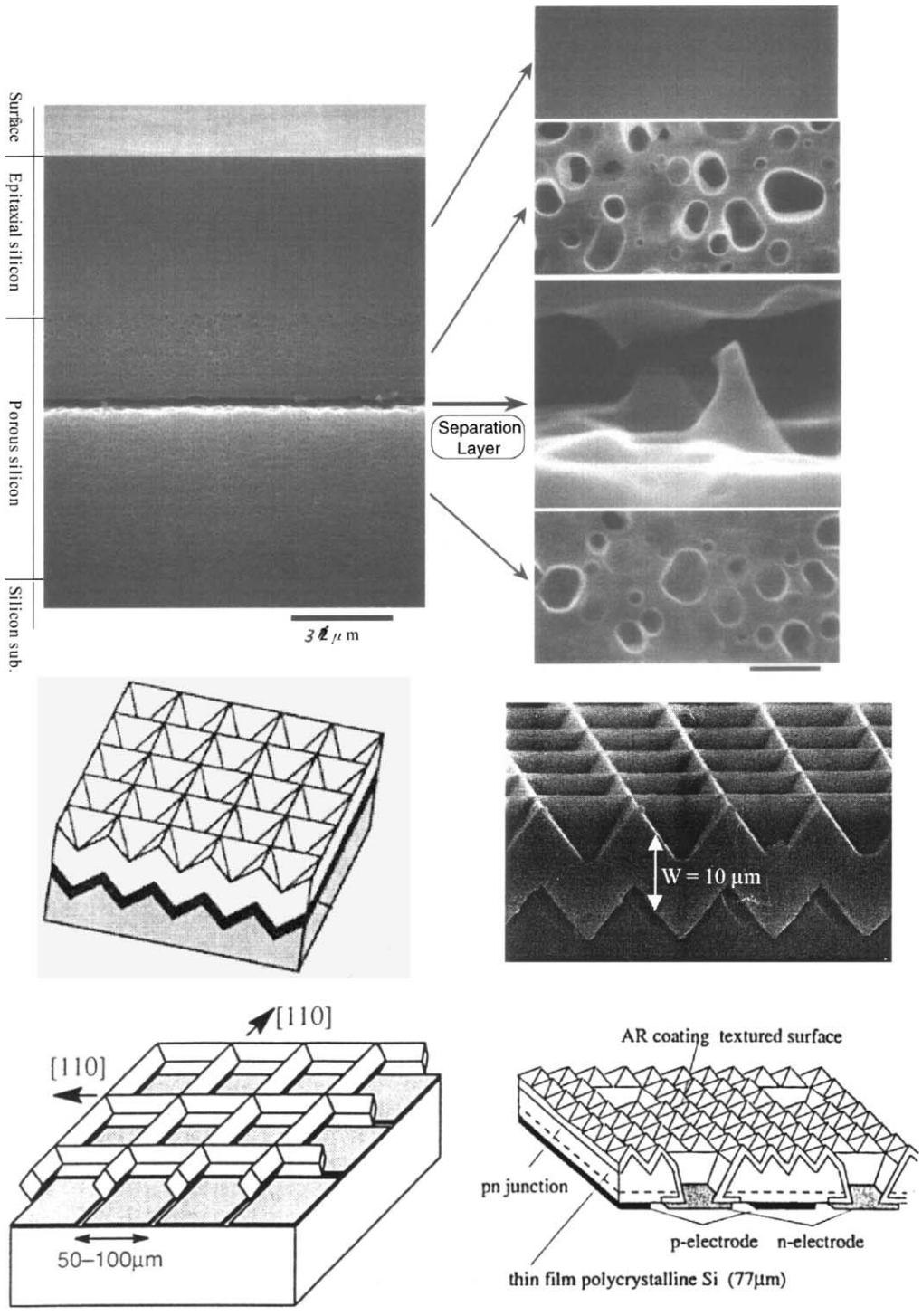

Fig. 21. Schematic of the most advanced transfer-techniques of monocrystalline Si-films: separation by porous layer formation (top) [85], Ψ-process (middle) [87], epi-lift process (bottom left) [88], VEST-process (bottom right) [84].

this kind of solar cells (so called Staebler–Wronski effect) [117]. Today, a-Si has its fixed place in consumer applications, mainly for indoor use. After understanding and partly solving the problems of light induced degradation amorphous silicon begins to enter the power market. Stabilized cell efficiencies reach 13%. Module efficiencies are in the 6–8% range. The visual appearance of thin-film modules makes them attractive for facade applications. An analysis by Suntola in 1992 predicted a stabilized module efficiency of 8% by the turn of the century [118]. This prediction appeared pessimistic at that time, however, this performance is still difficult to achieve on a production level. The present developments appear to sustain the contribution of this technology to large scale photovoltaics.

5.2. Properties and deposition techniques

Amorphous silicon is an alloy of silicon with hydrogen. The distribution of bond length and bond angles disturbs the long range of the crystalline silicon lattice order and consequently changes the optical and electronic properties. The optical gap increases from 1.12 to about 1.7 eV.

The effective energy gap of amorphous Si with respect to diffusion potential and—consequently—with respect to photovoltage in pn- and pin-structures is smaller than the effective bandgap for light absorption. The edges of the valence and conduction band are not well defined but exhibit a change in density of states. Charge carrier transport can occur at the mobility edge at energy levels which have still low absorption. This causes a material-inherent reduction of maximum obtainable efficiency. Furthermore, dangling bonds form deep levels in the forbidden gap of the material.

Basis for all deposition processes is silane as precursor gas in a chemical vapor deposition (CVD) process. Sputtering is not the method of choice for active semiconductor layers also in the case of amorphous silicon. Typical deposition temperatures are below 500 °C, otherwise no hydrogen is incorporated in the film. At low substrate temperature pre dissociation of the SiH_4 molecule is essential. The most commonly used method is plasma enhanced chemical vapor deposition (PECVD). Besides a variety of designs of the plasma reactor (diode, triode configurations) a range of frequencies from radio frequency (RF) to ultra high frequencies (UHF) is applied. Modification like remote plasma reactors, where dissociation is spatially separated from deposition or dissociation by an electron cyclotron resonance reactor (ECR) or a hot wire (HWCVD) have an influence on film quality.

The challenge is to produce a material with well defined disorder, which is a contradiction in itself. Therefore, the light induced defect modification cannot be completely avoided. It turns out that the stability of the material is related to the hydrogen content and not so much the process itself. The best quality is reached by diluting SiH_4 with hydrogen. It appears that a-Si:H has reached a state where further improvement of the material itself is not very likely. The hope was that HWCVD could yield a substantially more stable material. Early results in hot wire CVD gave hope to improve material stability, however, development of solar cells from this material did not lead to advantageous properties.

Improvements of solar cells now have to rely mostly on device design. Manufacturability may be improved by increasing deposition rate while maintaining sufficient material quality.

Hydrogen dilution allows to control the structure of the film. At very high dilution (<90%), a transition to the microcrystalline state of the material occurs. The bandgap of the μc material approaches that of crystalline silicon. Due to internal scattering the apparent optical absorption is nearly one order of magnitude higher compared to the crystalline material. Due to passivation by the high hydrogen content grain boundaries do not have a strong influence on device performance.

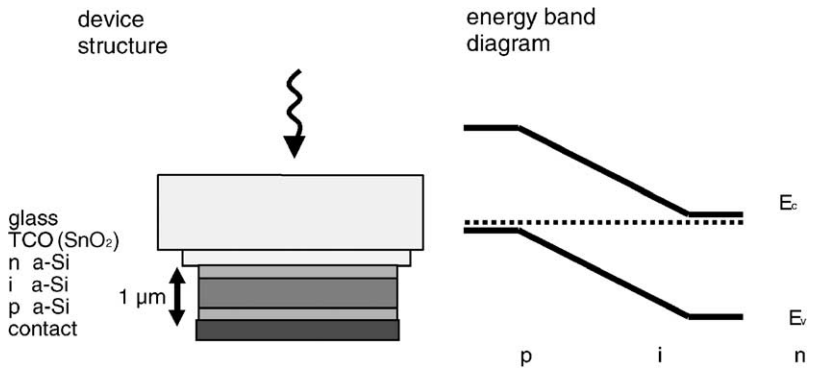

Fig. 22. Schematic structure of an amorphous pin solar cell and corresponding band structure.

5.3. Solar cell and module properties

The mobility of charge carriers in amorphous silicon is generally quite low so that collection of photogenerated carriers has to be supported by an internal electrical field. Furthermore, defect formation is related to the recombination process. The typical structure and the corresponding band diagram of an amorphous silicon solar cell is depicted in Fig. 22.

In order create a high field in the intrinsic layer of the pin structure the cells have to be thin, of the order of a few hundred nanometers. By applying proper light trapping schemes, thin single junction cells can be produced with high stabilized efficiency [119].

Therefore, the general strategy to improve the stabilized efficiency of the devices is to use a stack of two cells or even three cells. It allows to reduce the thickness of the single cells and, thus, to increase the electric field and, hence, improve carrier collection. The relatively low substrate temperature for the deposition of the films has the advantage that the underlying layers are not affected by the subsequent deposition steps. Therefore, production of these stacks in a monolithic structure does not add too much deposition time so that additional processing cost are not substantially higher than for single cells. Introducing cells with different bandgaps in the stack results in a "real" tandem cell (see Section 9.1) which can make better use of the solar spectrum, and at the same time improve the stabilized efficiency of the devices. The bandgap can be increased by alloying with carbon. Solar cells are produced in both substrate and superstrate configurations. Both have their own advantages. Superstrate cells are deposited on transparent conductive oxide (TCO) coated glass substrates. By pattering the TCO layer, the cells and back contact, a monolithic integration of cells on one large area substrate is possible. Substrate cells allow the use of flexible metal or polymer foils [120]. However, monolithic series connection requires an insulating substrate. Therefore cells on stainless steel substrates are usually cut into single cells and interconnected mechanically. The schematic view of a triple tandem cell on a stainless steel substrate produced by United Solar is shown in Fig. 23.

5.4. Status and future prospects

Two recent top values for the efficiency of a-Si based solar cells are presented in Table 2. The devices consist of either two or three cells in a stack. The second line gives data for the microcrystalline device fabricated by IMT Neuchatel based on amorphous semi-conductors.

Different approaches to a-Si module manufacturing are listed in Table 3. Module manufacturing of amorphous silicon follows mainly two lines, namely flexible foil substrates or glass substrates.

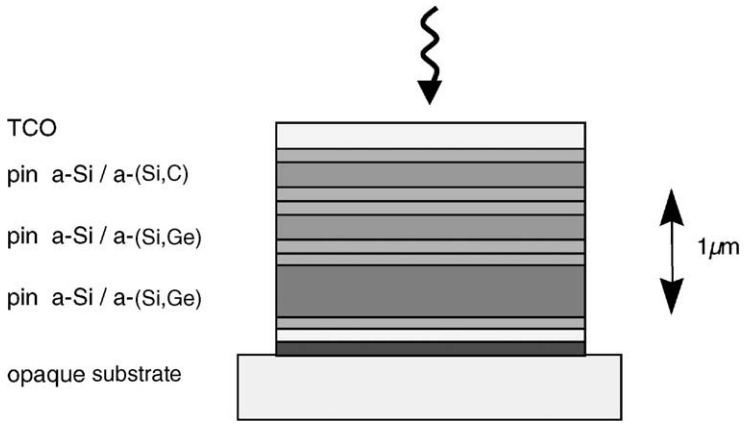

Fig. 23. Structure of a substrate type amorphous silicon tandem solar cell.

Table 2
Efficiencies (initial and stabilized) reached with laboratory scale devices based on amorphous semiconductors

Cell/type	Efficiency (initial/stabilized, %)	Manufacturer
a-Si/a-SiGe/a-SiGe	15.6/13.0	United Solar [121]
a-Si/μc-Si	13.1/10.7	IMT Neuchatel [122]

The flexible substrates offer new applications. However, monolithic interconnects of these cells are a challenging task.

Typical substrate sizes are in the order of 0.5–1 m^2. Stabilized efficiencies of large area modules are about 6–8% for multijunction cells and optimized single junction cells. The near term goal is to reach 8% stabilized efficiency on large areas on a production level. United Solar modules contain subcells which are laminated to a single cover sheet. The very large module of EPV consists of four submodules laminated to a single cover glass. The setup of the production of modules on the multimegawatt level is presently going on at United Solar and Solarex and Kaneka. Other companies operate pilot production lines for large area modules and are planning upscaling of the manufacturing lines.

Progress in amorphous silicon development is related to the following areas:

- General understanding of the material and of the stability issues. The understanding of the mechanism of the Staebler–Wronski effect being basically an intrinsic property of the material which adjusts its defect equilibrium according to the operating conditions.

Table 3
Different approaches to a-Si module manufacturing

Module type	Size/production volume	Company
a-Si, a-Si, a-SiGe, flexible stainless steel	Stainless steel foils, 5 MW	United Solar [121]
Double a-Si, a-SiGe, glass	0.46 m^2, 10 MW	Solarex
a-Si, a-Si, flexible, polymer	40 cm × 80 cm	FUJI
a-Si, glass	91 cm × 45 cm, 20 MW	Kaneka [119]
a-Si, a-Si, glass	0.6 m^2, 1 MW	ASE, PST

- Improvement of the process by hydrogen dilution of silane in the plasma discharge and very high frequency plasma deposition leads to improved material properties also at higher deposition rates.
- Understanding of structural properties of the material at the borderline between amorphous and crystalline state, so-called ''protocrystalline'' Si.
- Optimized cell designs by introducing buffer layers, alloy and doping gradients, etc. increase cell efficiency and reduce the effect of initial degradation.
- Optimized stacked cells and tandem devices lead to the highest stabilized efficiencies.

The ''classical'' approach uses an alloy with Ge to reduce the bandgap in the bottom cell(s) to about 1.5 eV. However, the corresponding process gas GeH_4 substantially contributes to the cost of the module, so that an alternative development for the low bandgap cell is advisable. One promising solution is the use of microcrystalline silicon. IMT Neuchatel demonstrated such a solar cells based on microcrystalline silicon [123]. The stable efficiency of over 8% reached till now may be low for a stand alone thin-film cell. However, in the so called ''micromorph concept'', i.e. a micromorph tandem concept, this cell could replace the Si, Ge bottom cell. The open circuit voltage of such microcrystalline cells is below 0.5 V so far. The electronic quality of the material depends strongly on the purity of the gases used in the process. Further investigations are needed to identify the limiting factors for solar cells based on this material.

The deposition of amorphous silicon at very low substrate temperatures below 100 °C still yields devices with reasonable efficiencies [124].

6. a-Si/c-Si heterostructures

A very interesting new development is the combination of crystalline and amorphous technologies in heterostructures. Absorption of sunlight still occurs mainly in a wafer of mono or polycrystalline silicon. The silicon wafer is contacted on both sides with amorphous silicon films. The principle is shown in Fig. 24. This technique represents a combination of c-Si and a-Si technologies.

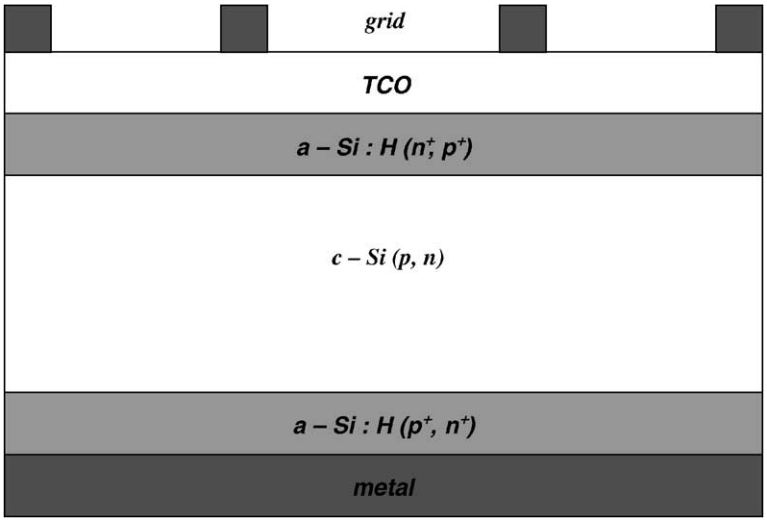

Fig. 24. Cross-section of an a-Si/C-Si/a-Si heterostructure.

This configuration has the following advantages:

- potential for high efficiency;
- very good surface passivation? Low surface recombination velocity;
- low processing temperatures? All processing steps occur below 200 °C;
- low thermal budget for processing? Reduction of energy pay back time;
- reduced cost of cell technology.

The best results with this approach were obtained by the Japanese company Sanyo. The latest achievement is a conversion efficiency of 20.7% for a cell area of 101 cm^2 using n-type Cz-silicon as the base (light absorbing) part [125]. Sanyo has developed the heterojunction with intrinsic thin layer (HIT)-structure. Its composition is a-Si(p^+)/a-Si(i)/c-Si(n)/a-Si(i)/a-Si(n^+). Very crucial in this structure is a thin intrinsic a-Si layer contacting the c-Si on both surfaces. This is apparently important for achieving good surface passivation. Interesting is that the crystalline silicon is n-type material. In this way as a side effect the instability described in Section 2.3 is avoided. Because of the low conductivity of a-Si a front window layer of a transparent conductor is required.

According to the information provided by Sanyo the solar cells have excellent stability. Sanyo has announced that pilot production of this type of cell is already under way.

7. Copper indium diselenide and related compounds

7.1. History

A very challenging technology is based on the ternary compound semiconductors $CuInSe_2$, $CuGaSe_2$, $CuInS_2$ and their multinary alloy $Cu(In,Ga)(S,Se)_2$ (in the further text: CIGS). The first results of single crystal work on $CuInSe_2$ (CIS) [126] were extremely promising but the complexity of the material looked complicated as a thin-film technology. Pioneering work of Kazmerski et al. [127], however, showed immediate success. It became evident that CIS process technology is very flexible with respect to process conditions. Establishing a well controlled system for multisource coevaporation by Boeing made the CIS cell soon the front-runner with respect to thin-film solar cell efficiencies. ARCO Solar developed in the mid-1980s, a fabrication technology which is more adapted to current thin-film processing, namely sputtering of metal films with a subsequent selenisation step [128]. In later developments the addition of Ga and S helped to increase the efficiency.

7.2. Material properties and deposition techniques

The phase composition of the ternary compound is mostly described by the pseudo-binary phase diagram of the binary Cu_2Se and In_2Se_3 phase. Recent investigations by Haalboom et al. [129] showed that single phase chalcopyrite $CuInSe_2$ only exists at a small copper deficiency. In Indium rich films defect chalcopyrite phases segregate. Nevertheless, the electronic properties of the compound are not very much affected by deviation from stoichiometry. A plausible explanation was derived from theoretical calculations [130]. Cu vacancies form together with In interstitials a neutral defect complex: $2(V_{Cu})^- + (In_{Cu})^{2+}$.

The energy levels of this complex lie in the valence or conduction band. Furthermore, these chalcopyrite semiconductor compounds form a Cu depleted defect layer at the surface [131,132]. This behavior has important consequences for junction formation because it forms a type inversion at the surface of the p-type film.

The importance of sodium for the quality of CIGS films became more and more evident. Sodium not only improves crystallization of the film but also increases conductivity. The mechanism is still not known. There is much evidence that sodium is incorporated at grain boundaries or defects. Concentration of Na in the bulk must be very low [133].

For the large scale fabrication of these rather complex compounds two different approaches or even philosophies exist for the deposition of the absorber layer:

- Deposition of precursor layers and a subsequent treatment or annealing in H_2Se vapor. The process is divided in several simple steps. These processes can use "off the shelf" equipment as far as possible and therefore need in principle only the process development. However, this strategy had limited success till now. Furthermore it limits the composition of the absorber layer to low bandgap In rich material.
- Taking the process which yields the best performance on small area laboratory scale devices namely coevaporation. This procedure gives full flexibility in device optimization. However, it is a real challenge for the engineers to design appropriate evaporation sources while achieving somehow the guarantee of high efficiency upscaling.

Fig. 25 illustrates the different methods for CIGS film deposition. A careful analysis and future experience has to show which option is most suitable for upscaling. The addition of several simple steps could be less economic than one sophisticated but efficient process. Deposition speed of in-line coevaporation can be as high as 5 cm/min with the presently known parameters and source design. This means a module with the length of 1 m could be deposited in 20 min (Table 4).

The cells produced by the selenization process contain gallium only towards the back of the cells, because of the principal difficulty to incorporate this element homogeneously in the film during this process. Therefore the bandgap towards the surface is widened by introducing sulfur forming a graded bandgap structure.

The selenisation technique is now the basis of the first pilot production and market introduction of CIS-modules by Siemens Solar. Aperture area efficiencies of over 12% make these modules attractive for power applications [135]. Evaporation processes for compounds consisting of four

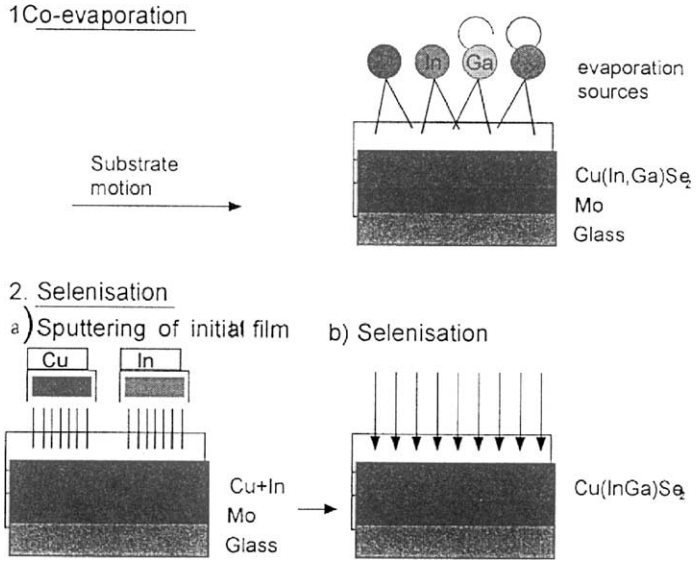

Fig. 25. Comparison of approaches: selenization of metallic precursors vs. coevaporation.

Table 4
Deposition of CIGS films module manufacturing

Deposition method	Company
Metal precursor + H_2Se selenization	Siemens Solar Industries (SSI), Showa Shell [135]
Metal/Se precursor, anneal	Siemens Solar [136]
Metal precursor no vacuum	ISET, Unisun [137]
Coevaporation	ZSW [137], Gobal Solar [139]

elements like $Cu(In,Ga)Se_2$ on large areas have been considered as unsolvable problems. However, based on the long-term experience at IPE dating back to the CdS deposition, the Center for Solar Energy and Hydrogen Research (ZSW) demonstrated coevaporation processes on 60 cm wide glass substrates [139,140]. Global Solar [138] is depositing the cell in a continuous process on a stainless steel or polymer web. Since vacuum deposition systems require high investments, other methods like particle deposition are under investigation.

7.3. Solar cell and module properties

CIGS module fabrication has the same advantageous features of thin-film fabrication processes as the other thin-film solar cell materials. The typical device structure shown in Fig. 26 is based on a soda lime glass substrate which often also serves as a source for the doping of the CIGS films with sodium. Typical solar cells are deposited on Mo coated glass substrates at a substrate temperature above 500 °C. The heterojunction is formed by chemical deposition of a thin CdS layer from a solution containing Cd-ions and thiourea as a sulfur source. This process has many intrinsic advantages so that it is difficult to replace it by either another Cd-free compound or a more convenient gas phase process [133]. The most efficient devices and first large scale productions of modules still rely on the CdS layer. However, research in many labs concentrates on the replacement of the CdS layer. One effort in Japan includes a wet deposited Zn(S,OH) compound already in pilot production [134].

Attempts to realize superstrate cells like with CdTe or a-Si are hampered by the high deposition temperature for the CIGS film resulting in a non-controllable interdiffusion at the heterojunction. Therefore the efficiency of these devices is limited to 10% [141].

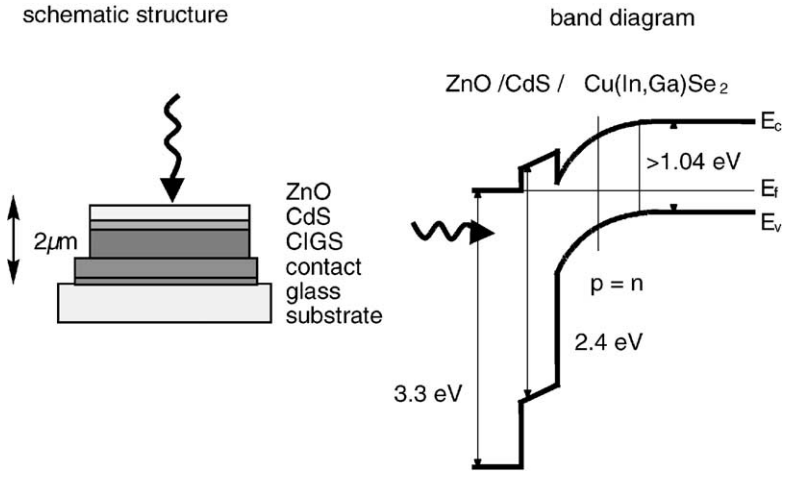

Fig. 26. Schematic structure of a CIGS-based solar cell.

Table 5
Performance of CIGS cells and modules

Process	Laboratory cell efficiency (%)	Module efficiency (%)/area (cm^2)	Laboratory/company status
Selenization of precursor	>16	12.1/1 × 4 ft[a]	Siemens, pilot production
Metal films	–	14.7/18[b]	–
Coevaporation/sequential evaporation	18.8	–	NREL [143]
	17.2	13.9/90[b]	IPE [144]
	16.2	12.7/800[b]	ZSW, laboratory production; Würth Solar, pilot production
	–	9.6/135[a]	EPV
	11.5	5.6/240	Global Solar [139]
	–	16.8/19[b]	Angstrom Solar Center [145]
Non-vacuum processes	>11	8/74	ISET [146], Unisun [147]

[a] Independently confirmed at NREL.
[b] Independently confirmed at ISE/Fraunhofer.

7.4. Status and future prospects

Very high efficiencies approaching 19% have been reported for laboratory scale devices [142]. This result has been obtained by this material system by empirical optimization of process parameters. Due to the high flexibility of designing compounds with defined properties in this material system (e.g. bandgap grading), even more improvements can be expected in the near future. Table 5 summarizes the best values of solar cell performance obtained by this material system.

A further challenge is to realize high voltage devices also on the basis of the ternary chalcopyrite compounds $CuInS_2$ and $CuGaSe_2$. The efficiency achieved with these wide energy gap materials are still considerably lower than those of the low gap $Cu(In,Ga)Se_2$ [147–149]. This limitation is mostly due to the low open circuit voltage compared to the bandgap. However, improved understanding of the materials, especially the surface and junction properties may help to further develop the devices in the near future and open new perspectives of ternary thin-film photovoltaic devices. Further developments are directed towards replacement of the CdS buffer layer and probably the reduction of film thickness or even replacement of In and Ga as rare elements [150].

8. Cadmium telluride

8.1. History

Thin-film solar cells based on CdTe are the cells with the longest tradition, but they are really not ''of age''. After a long steeplechase they arrived at cell efficiencies of 16% and large-area module efficiencies of over 10%. There is no reason why they should not improve further in the foreseeable future. The history of CdTe-based cells is a story about an adventurous search for the appropriate structure on a track full of obstacles and traps. As in the case of CdS, first attempts have been made with CdTe single crystals. At the RCA Labs, indium was alloyed into n-type CdTe crystals resulting in an alloy-type pn-junction with 2.1% conversion efficiency. At the same time, CdTe-cell efficiencies of even 4% were published in the USSR and submitted for publication even! Cusano reported on the first thin-film cell; he used a structure similar to the CdS cells, namely

a p-Cu_2Te/n-CdTe heterojunction, and succeeded in obtaining 6% efficiency, an excellent value for the first trial at that time [151]. For 9 years after the work reported by Cusano, there was not much to report about this material. In this interval CdTe was used as p-type material in conjunction with n-CdS, not only for testing pn-heterojunctions, but also for producing graded-gap junctions by interdiffusion of the materials. Achieving not more than 6% efficiency, the researchers saw the first two of three dominant problems of CdTe solar cell development:

- the difficulty of doping p-type CdTe,
- the difficulty in obtaining low-resistance contacts to p-type CdTe, and the recombination losses associated with the junction interface.

In the years to come more than 10 different types of solar cell structures with CdTe as the absorber have been tested (see e.g. [152–154]). The borderline of 10% efficiency was crossed in 1982, astonishingly again with a n-CdS/p-CdTe heterojunction made in the labs of Kodak [155]. Furthermore, the cell featured only a very thin CdS-layer that improved the blue response. Very thin CdS-layers, acting only as a buffer layer in the heterostructure with the transparent conductive oxide—see also $CuInSe_2$-cells—were the key to further improvements. The research groups at the National Renewable Laboratory and at the University of South Florida (USF) [156] are those having pushed the efficiency to the range of 16%. Doping is thought to be related to $[V_{Cd}\text{-}Cd_{Te}]$ while oxygen and background impurities like copper might also play a role.

A large number of deposition methods have been applied for CdTe, resulting in high-quality layers and high-efficiency cells on the one hand and in economic production on the other hand. Close spaced sublimation (CSS) is the most popular technique for obtaining highest efficiencies, spraying or screen printing are techniques with high economic potential. It is remarkable that the highest efficiency CdTe PV devices are fabricated from polycrystalline rather than single crystalline CdTe. According to [157], a fundamental question therefore is ‘‘why are polycrystalline thin-film PV devices more efficient than their single crystal counterparts?’’. A possible answer is that grain boundaries *enhance* the collection of photogenerated minority carriers! There are indications that an electron barrier exists at grain boundaries [158] that makes devices fabricated from II–VI compounds generally less sensitive to grain boundaries than are devices made from III–V or group IV materials.

8.2. Material properties and deposition techniques

CdTe is a nearly ideal material for thin-film photovoltaics because it combines several advantageous properties. Besides an optical bandgap close to the optimum for solar energy conversion it is very easy to handle in thin-film deposition processes. Therefore, many efforts were and still are directed towards the large scale fabrication of modules. Laboratory cells reach efficiencies above 16% [157].

The congruent evaporation of the compound, i.e. the evaporation of stoichiometric CdTe results in a stoichiometric composition of the vapor. Above a substrate temperature of a few hundred degree Celsius, the composition is self stabilizing. High quality material can be deposited at very high rates (>1 μm/min) at substrate temperatures of 450–600 °C. Because of the tolerance of the material to defects and grain boundaries, simple processes such as electrodeposition and screen printing are possible and these processes are a good prerequisite for large scale production. The highest quality material and, hence, the highest efficiencies are obtained with close spaced sublimation (CSS), a modified evaporation process, where substrates and sources are very close together with a relatively small difference in temperature so that the film growth occurs close to equilibrium condition (Fig. 27).

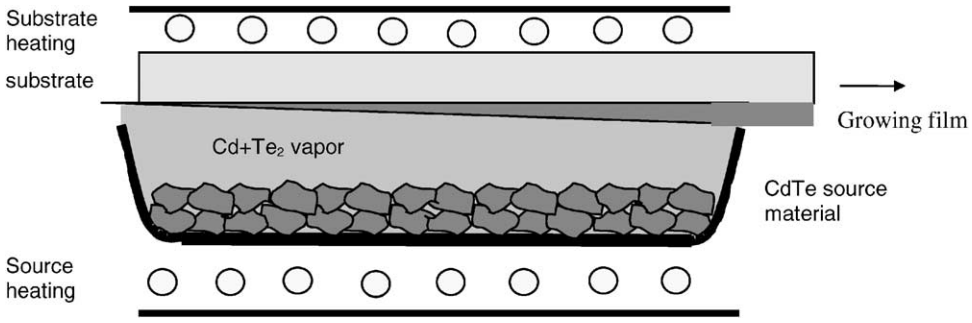

Fig. 27. Schematic view of a reactor for the continuous deposition of CdTe by close spaced sublimation.

Table 6
Approaches to CdTe module manufacturing, all companies fabricate modules with sizes >0.5 m^2

Deposition technique	Status, companies
Close spaced sublimation	Production started First Solar, ANTEC, Matsushita
Modified close spaced sublimation	
Electrodeposition	Pilot production, multimegawatt planned by BP Solar [159]
Screen printing	Matsushita

The different methods for CdTe deposition in Table 6 gives an impression of the flexibility of the material with respect to manufacturing. In line processes with high deposition speed (CSS) or processes where large batches can be handled (electrodeposition) have been developed. All the companies involved in CdTe development plan upscaling and a multimegawatt production in the near future.

8.2.1. Solar cell and module properties

The active layers of a CdTe based solar cell are deposited on TCO (SnO_2 or indium tin oxide) coated glass like in a-Si superstrate cells. High efficiency cells use very thin chemically deposited CdS (see also CIGS based cells). In line processes by closed spaced sublimation usually include CdS deposition. In this case the CdS layer has to be thicker for a good coverage of the substrate. Therefore, losses in the CdS window are increased. The schematic structure of the typical CdTe-based solar cell is shown in Fig. 28.

CdTe–CdS solar cell fabrication includes the following major technical issues:

- junction formation,
- crystallization of the films,
- formation of stable back contacts.

The fabrication of the heterojunction is one of the keys to efficient devices. Due to the intermixing of the CdS and the CdTe layer, not an abrupt heterojunction but a graded gap structure is formed. Interdiffusion of the CdS and CdTe layers during fabrication or after a $CdCl_2$ treatment determine the electrical properties of the device. The $CdCl_2$ treatment of the CdTe film which is universally used also enhances the size of the crystallites in small grained polycrystalline films. The fabrication of stable ohmic contacts to the wide gap p-type semiconductor CdTe is a prerequisite for stable modules. Complex recipes for contact formation include chemical treatments for creating a Te-rich surface combined with the deposition of Sb, Carbon or Cu.

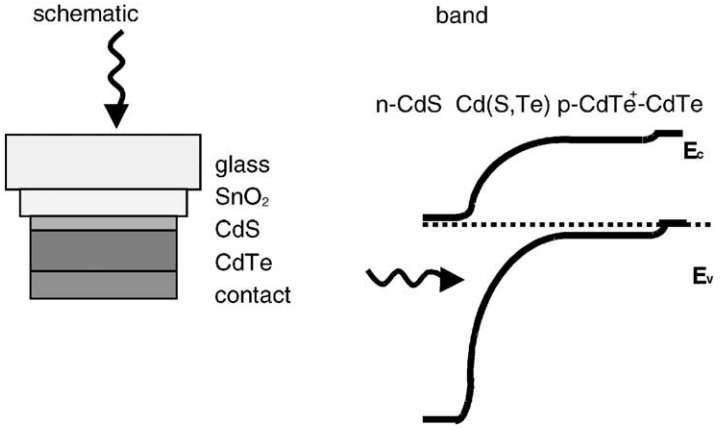

Fig. 28. Schematic structure of a CdTe-based superstrate solar cell.

8.3. Status and future prospects

At present there are several attempts to set up production lines for CdTe based modules with capacities in the multimegawatt range. The activities of the different companies are listed in Table 6. The area of monolithic thin-film modules approaches one square meter. The monolithic thin-film module with the worlds highest power output has been produced based on CdTe. At BP Solarex, a monolithic module with a power output exceeding 70 W has been fabricated [159]. In this case, the CdTe layer has been electrodeposited. First Solar attempts to connect solar cell production to a float glass line. The future has to show in how far sophisticated processing can be translated to large area high-throughput production.

A non-technical problem associated with CdTe is the acceptance in the market place because Cd and to a lesser extent Te are toxic materials although the compound is quite stable and harmless.

9. Other materials and concepts

9.1. Tandem cells, concentrating systems

The efficiency of solar cells can be significantly increased by stacking several cells with different bandgaps such that the gap energy decreases from the top. Then each solar cell converts part of the solar spectrum at maximum efficiency. Two cells in series connection have a maximum theoretical efficiency of 41.9% and with a larger number of cells 50% can be exceeded. Such tandem arrangements can be realized either with a sequence of thin-films as has already been demonstrated with amorphous silicon or they can be incorporated into concentrating systems. A problem connected with tandem cells is that with series connected cells an equal number of photons has to be absorbed in each cell. If at all this can only be accomplished at one spectral distribution like AM1.5. Since this distribution changes in terrestrial applications, spectral mismatch will occur. An obvious but complex solution is to provide separate contacts to each cell.

Concentration of sun light is an approach complementing III–V cells in order to reduce the cost of conversion. It is only feasible with direct sunlight which is concentrated by optical elements tracking the sun. If the concentration factor is very high, then the cost of the solar cell is only a small

part of systems cost and therefore the solar cells can be expensive as long as efficiency is very high. For this purpose even high cost III–V compounds are possible including tandem systems. Concentration of radiation leads also to increased efficiency since V_{oc} is proportional to the logarithm of light generated current density. These tandem cells are now in the process of being introduced into the space (satellite) market [160].

9.2. Dye-sensitized cells

Nano-crystalline dye sensitized solar cells are based on the mechanism of a fast regenerative photoelectrochemical process. The main difference of this type of solar cells compared to conventional cells is that the functional element which is responsible for light absorption (the dye) is separated from the charge carrier transport itself. In the case of the n-type semiconductor TiO_2 (bandgap 3.2 eV), this results in a working cycle starting with the dye excitation by an absorbed photon at the TiO_2/electrolyte interface and an electron injection into the TiO_2. The injected electrons may migrate to the front electrode (a transparent TCO glass) and can be extracted as an external current. The dye is subsequently reduced by a redox electrolyte, based on an organic solvent and the redox couple iodide/triiodide. The redox electrolyte also accomplishes the charge transport between the counter electrode (also a TCO glass) and the dye molecules. For a low-resistant electron transfer, the counter electrode is covered with some Pt which acts as a catalyst for the redox reaction).

It could be shown that only dye molecules directly attached to the semiconductor surface are able to efficiently inject charge carriers into the semiconductor with a quantum yield of more than 90%. As the overall light absorption of a dye monolayer is only small, this limits the photocurrent efficiency with respect to the incident light to a value well below 1%. This mechanism could be evaded by the preparation of titaniuim dioxide electrodes with a nanoporous morphology resulting in a roughness factor of about 1000 [161]. After the announcement of surprisingly high efficiencies by O'Regan and Grätzel in the early-1990s [162], this type of solar cell is under reinforced development aiming at large area and low cost solar cells [163]. After the first experimental success, it took nearly a decade until the first quantitative models were established which link the material parameters of the constituents with the electrical performance of the whole cell such as the *I–V* characteristic and the spectral response [164].

The major advantage of the concept of dye sensitization is the fact that the conduction mechanism is based on a majority carrier transport as opposed to the minority carrier transport of conventional inorganic cells. This means that bulk or surface recombination of the charge carriers in the TiO_2 semiconductor cannot happen. Thus, impure starting materials and a simple cell processing without any clean room steps are permitted, yet resulting in promising conversion efficiencies of 7–11% and the hope of a low-cost device for photoelectrochemical solar energy conversion. On the other hand impure materials can result in a strongly reduced lifetime of the cells.

The most important issue of the dye-sensitized cells is the stability over the time and the temperature range which occurs under outdoor conditions. Although it could be shown, that intrinsic degradation can considerably be reduced, the behavior of the liquid electrolyte under extreme conditions is still unknown [165]. For a successful commercialization of these cells, the encapsulation/sealing, the coloration and the electrolyte filling has to be transferred into fully automated lines including the final closure of the filling openings [166]. Therefore, a significant effort is taken in order to replace the liquid electrolyte by a gel electrolyte, a solid-state electrolyte or a p-conducting polymer material. Using p-type conducting materials, best efficiencies obtained so far are in the 1% range [167]. Recently, high efficiencies above 7% were announced by Toshiba using a gel electrolyte [168].

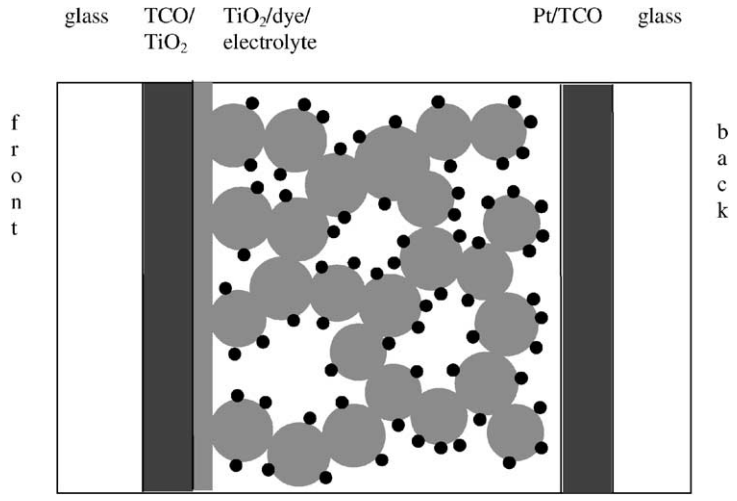

Fig. 29. Principle of the dye-sensitized solar cell.

In terms of a possible integration of these cells into electronic devices, the necessary sintering step of the nanometer-sized TiO_2 at temperatures of over 400 °C on the transparent conductive oxide (TCO) glass might be a certain drawback. Due to this thermal budget, the glass electrode is the only solution which limits the shape of the cells to a flat design (Fig. 29).

9.3. Organic solar cells

Beside dye-sensitized solar cells, which may be considered as organic/inorganic hybrid cells, other types of organic solar cells currently become of broader interest. These cells can be divided roughly into molecular and polymer organic solar cells [169], or into flat-layer systems and bulk heterojunctions [166].

Organic materials as, e.g. conjugated polymers, dyes or molecular organic glasses can show p- or n-type semiconducting properties. Extremely high optical absorption coefficients are possible with these materials, which offers the possibility for the production of very thin solar cells (far below 1 μm), and therefore, only very small amounts of needed materials. The variability of organic compounds is nearly infinite. Beside this, the large interest in these materials results from technological aspects as the expected ease of large-scale manufacturing at low-temperature processes and very low costs. The upscaling of organic solar cells into large-area devices, always a big challenge with inorganic solar cells, has already been demonstrated to be straightforward. The energetic pay-back time of organic solar cells is expected to be very short. Considering the fact that light emitting films of plastic materials have been realized there is a realistic chance to achieve efficient photovoltaic conversion also in such materials because this is just the reverse process. Organic solar cells offer the hope of being very inexpensive. Quite a variety of materials, compositions and concepts are being investigated, which reflects the possibilities in terms of device concepts, materials use and materials design. In spite of the many fundamental questions that still exist, these perspectives and the fact that exploration has only just begun, cause a largely growing interest in the development of such solar cells.

The width of the charge generation layer for organic solar cells is much smaller than in inorganic cells [170]. In order to overcome this obstacle, the concept of interpenetrating networks with modified fullerene (i.e. C_{60}) particles was successfully introduced by the Heeger group [183].

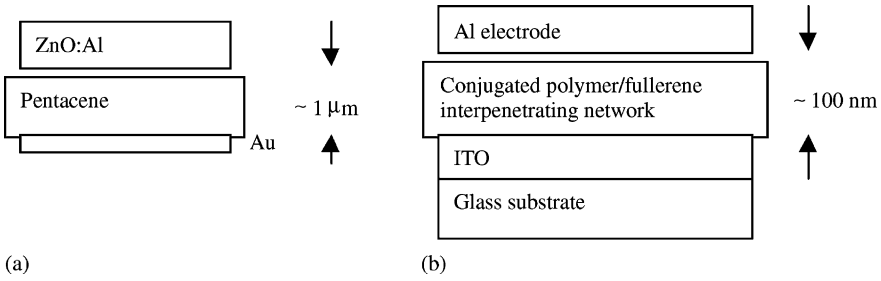

Fig. 30. Organic solar cells: single crystal heterojunction (a) and conjugated polymer/fullerene "plastic solar cell" (b).

Fullerenes have been proven to be very efficient electron acceptors for photoexcited conjugated polymers; the quantum efficiency for charge separation is near unity [171]. Mixtures of fullerene derivates (e.g. PCBM) and conjugated polymers (e.g. MDMO-PPV) are spin-coated or doctor-bladed on suitable substrates, such as ITO coated polymer foils or glasses. Interpenetrating networks can also be produced by co-evaporation of fullerenes and molecular dyes as, e.g. zinc phthalocyanine [172]. Another concept is the use of stratified layers made of donor–acceptor blends, avoiding the problem of continuous and separate pathways for the two types of charge carriers, which in interpenetrating networks might exist between anode and cathode [173].

Only modest solar conversion efficiencies of up to only 1% were reached until 1999. Efficiencies increased rapidly within this year: with molecular flat-layer systems based on molecular organic single crystals made of iodine or bromine doped pentacene, efficiencies of up to 3.3% under AM1.5 illumination have been reported at Lucent Technologies [174]. Nearly, the same value was reported with improved bulk heterojunctions (interpenetrating network) of conjugated polymers and fullerene derivatives.

Before these cells become practical, which at the moment looks still far away, the efficiency will have to be increased further. Also, long-term stability and protection against environmental influences are significant challenges (Fig. 30).

9.4. Theoretical concepts for new high efficiency semi-conductor materials

This section deals with new theoretical materials that do not yet exist but would offer significant advantages for photovoltaic conversion. They might be called designer materials. In principle they are designed to combine the effect of tandem cells in one material.

9.4.1. Auger generation material

In this concept, the higher energy photons (energy greater than $2E_G$) should generate two or even more electron hole pairs by impact ionization [104,175,176]. The maximum theoretical efficiency of such a material is 42% instead of 30% for a semiconductor with optimal gap. The requirements for the band structure of such a material have been worked out but no such material has yet been synthesized. According to [177], the new material should have a fundamental indirect gap of 0.95 eV and a direct gap at 1.9 eV. As a possible material a Si–Ge alloy has been identified.

A related concept is the hot carrier device in which carriers are collected before thermalization sets in [178,179].

9.4.2. Intermediate metallic band material

The intermediate metallic band material solves a problem that has a long history in solar cell materials design. Photons with energy less than the gap could be utilized if an intermediate energy

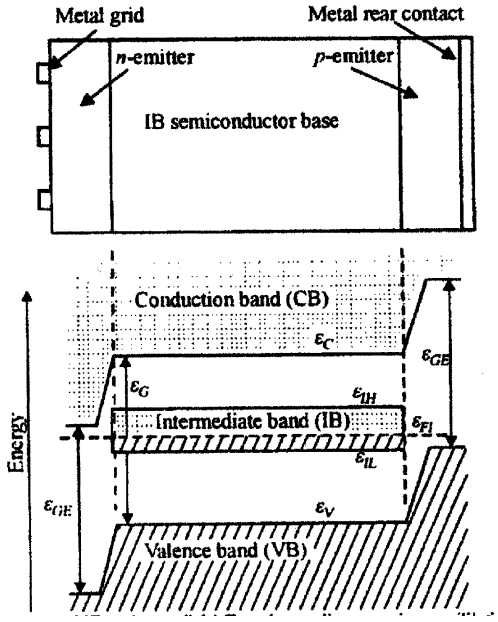

Fig. 31. Diagram of intermediate band solar cell.

level around midgap were present through which carriers could be transported from one band edge to the other by two photons. Unfortunately, such levels are also strong recombination centers and lead to drastic degradation of the material. This problem is circumvented (at least theoretically) by placing a narrow metallic band within the gap of a wide gap semiconductor [180,181] (Fig. 31). The intermediate band prevents non-radiative recombination. Both, holes and electrons exist as minority carriers and due to the metallic nature of the band, charge neutrality is always established. Optimum absorption edges should be at 0.93, 1.40 and 2.43 eV. The theoretical efficiency of this device is 46.0%, compared to 41.9% of the tandem cell described above. The intermediate band base material should be placed between two ordinary semiconductors, one strongly n-doped, the other strongly p-doped, as shown in Fig. 31. The metallic band would otherwise short circuit the device.

A proposal already exists how to manufacture the intermediate band material [182]. It is proposed to incorporate quantum dots of 35 to 70 Å diameter of a suitable ternary compound into another, wider gap ternary material. Whether this material can be synthesized, remains an open question.

10. Summary and outlook

We have tried to give an up to date perspective of PV materials. The most important material has been and still is silicon. It dominates the present world market, particularly in its crystalline form but amorphous silicon is also of importance. Silicon solar cells are still heavily dependent on the materials base of the semiconductor industry. Special types of crystallization are block casting and ribbon growing. Crystalline silicon still has a large potential for cost reduction in its conventional form and even more so in the crystalline thin-film version.

Great hope rests with the thin-film materials which require only small amounts of material. Amorphous silicon, cadmium telluride and copper indium gallium diselenide are the most hopeful materials.

A great number of new concepts and materials are still in the research stage. Some of them may lead to much higher efficiency and lower cost in the coming decades.

A long way is still ahead of photovoltaics before the goal, a sizable contribution to world electricity production is attained. However, the prospects of reaching this goal are good because so many different and promising materials and concepts have emerged.

References

[1] A.E. Becquerel, Comt. Rend. Acad. Sci. 9 (1839) 561.
[2] A. Goetzberger, J. Knobloch, B. Voss, Crystalline Silicon Solar Cells, Wiley, New York, 1998.
[3] M.A. Green, Silicon Solar Cells: Advanced Principles and Practice, Bridge Printery, Sidney, 1995.
[4] Shell Renewable Energy Information Brochure, 1997.
[5] D.M. Chapin, C.S. Fuller, G.L. Pearson, J. Appl. Phys. 25 (1954) 676.
[6] W. Zulehner, Mater. Sci. Eng. 4 (1989) 1–10.
[7] J. Palm, A. Lerchenberger, W. Kusian, W. Krühler, A.L. Endrös, G. Mihalik, B. Fickett, J. Nickerson, T. Jester, in: Proceedings of the 16th European PV Solar Energy Conference, Glasgow, 2000, p. 1222.
[8] H. Fischer, W. Pschunder, in: Proceedings of the 10th IEEE PV Specialists Conference, Palo Alto, CA, USA, 1973, p. 405.
[9] J. Knobloch, S.W. Glunz, D. Biro, W. Warta, E. Schaffer, W. Wettling, in: Proceedings of the 25th IEEE Photovoltaic Specialists Conference, Washington, DC, USA, 1996, pp. 405–408.
[10] T. Yoshida, Y. Kitagawara, in: Proceedings of the 4th International Symposium on High Purity Silicon IV, San Antonio, USA, 1996, pp. 450–454.
[11] J. Schmidt, A.G. Aberle, R. Hezel, in: Proceedings of the 26th IEEE Photovoltaic Specialists Conference, Anaheim, USA, 1997, pp. 13–18.
[12] S.W. Glunz, S. Rein, W. Warta, J. Knobloch, W. Wettling, in: Proceedings of the 2nd World Conference on Photovoltaic Energy Conversion, Vienna, Austria, 1998, pp. 1343–1346.
[13] S.W. Glunz, S. Rein, W. Warta, J. Knobloch, W. Wettling, Solar Energy Materials and Solar Cells 65 (2000) 212.
[14] J. Schmidt, A. Cuevas, J. Appl. Phys. 86 (1999) 3175–3180.
[15] S.W. Glunz, S. Rein, J. Knobloch, W. Wettling, T. Abe, Prog. Photovolt. 7 (1999) 446–463.
[16] T. Saitoh, X. Wang, H. Hashigami, T. Abe, T. Igarashi, S.W. Glunz, W. Wettling, A. Ebong, B.M. Damiani, A. Rohatgi, I. Yamasaki, T. Nunoi, H. Sawai, H. Ohtuka, Y. Yazawa, T. Warabisako, J. Zhao, M.A. Green, Technical Digest of the 11th International Photovoltaic Science and Engineering Conference, Sapporo, Japan, 1999, pp. 553–556.
[17] L.C. Kimerling, M.T. Asom, J.L. Benton, P.J. Drevinsky, C.E. Caefer, in: Proceedings of the 15th International Conference on Defects in Semiconductors, Budapest, Hungary, 1988, pp. 141–150.
[18] S.W. Glunz, S. Rein, J. Knobloch, in: Proceedings of the 16th European PV Solar Energy Conference, Glasgow, 2000, p. 1070.
[19] J. Zhao, A. Wang, M.A. Green, Prog. Photovolt. 7 (1999) 471–474.
[20] S.W. Glunz, J.Y. Lee, S. Rein, in: Proceedings of the 28th IEEE Photovoltaic Specialists Conference, Anchorage, Alaska, USA, 2000, p. 201.
[21] S.W. Glunz, B. Köster, T. Leimenstoll, S. Rein, E. Schäffer, J. Knobloch, T. Abe, Prog. Photovolt. 8 (2000) 237–240.
[22] J. Dietl, D. Helmreich, E. Sirtl, Crystals: Growth, Properties and Applications, vol. 5, Springer, Berlin, 1981, p. 57.
[23] A. Goetzberger, W. Shockley, J. Appl. Phys. 31 (1960) 409.
[24] M.A. Green, et al., Prog. Photovolt.: Res. Appl. 7 (1999) 31.
[25] C. Gerhards, A. Fischer, P. Fath, E. Bucher, in: Proceedings of the 16th European PV Solar Energy Conference, Glasgow, 2000, p. 1390.
[26] A.R. Burgers, J.H. Bultman, C. Beneking, W.A. Nositschka, O. Voigt, H. Kurz, in: Proceedings of the 16th European PV Solar Energy Conference, Glasgow, 2000, p. 1427.
[27] D.S. Ruby, S.H. Zaidi, S. Narayanan, in: Proceedings of the 28th IEEE Photovoltaic Specialists Conference, Anchorage, Alaska, USA, 2000, p. 75.
[28] S. De Wolf, R. Einhaus, K. De Clercq, J. Szlufcik, in: Proceedings of the 16th European PV Solar Energy Conference, Glasgow, 2000, p. 1521.
[29] R. Lüdemann, B.M. Damiani, A. Rohatgi, in: Proceedings of the 28th IEEE Photovoltaic Specialists Conference, Anchorage, Alaska, USA, 2000, p. 299.
[30] A. Goetzberger, in: Proceedings of the 26th IEEE PV Specialists Conference, Anaheim, USA, 1997, p. 1.
[31] H.-D. Block, G. Wagner, in: Proceedings of the 16th European PV Solar Energy Conference, Glasgow, 2000, p. 1059.

[32] H. Nussbaumer, Herstellung und Eigenschaften rekristallisierter Siliziumschichten, Dissertation, University of Konstanz, 1996.
[33] T.F. Ciszek, J. Crystal Growth 66 (1984) 655.
[34] A. Eyer, A. Räuber, A. Goetzberger, Optoelectron.-Dev. Technol. 5 (2) (1990) 239.
[35] R.B. Bergmann, J.H. Werner, Kristallzüchtung für die Photovoltaik—Forschung in Deutschland, Mitteilungsblatt der Deutschen Gesellschaft für Kristallwachstum und Kristallzüchtung, vol. 59, 1994, p. 15F.
[36] J.P. Kalejs, B.H. Mackintosh, E.M. Sachs, F.V. Wald, in: Proceedings of the 14th IEEE Photovoltaic Specialists Conference, San Diego, 1980, p. 13.
[37] F. Wald, Crystals, Growth, Properties and Applications, vol. 5, Springer, Berlin, 1981, p. 157.
[38] W. Schmidt, B. Woesten, in: Proceedings of the 16th European PV Solar Energy Conference, Glasgow, 2000, p. 1083.
[39] B.H. Mackintosh, M.P. Quellette, B.P. Piwczyk, M.D. Rosenblum, J. Pl Kalejs, in: Proceedings of the 28th IEEE Photovoltaic Specialists Conference, Anchorage, Alaska, USA, 2000, p. 46.
[40] W. Schmidt, B. Woesten, in: Proceedings of the 16th European PV Solar Energy Conference, Glasgow, 2000, p. 1083.
[41] T.F. Ciszek, J.L. Hurd, M. Schietzelt, J. Electrochem. Soc. 129 (12) (1982) 2823.
[42] T.F. Ciszek, in: C.P. Khattak, K.V. Ravi (Eds.), Silicon Processing for Photovoltaics, Elsevier, Amsterdam, 1985.
[43] R.L. Wallace, J.I. Hanoka, S. Narasimha, S. Kamra, A. Rohatgi, in: Proceedings of the 26th IEEE Photovoltaic Specialists Conference, Anaheim, 1997, p. 99.
[44] R. Janoch, R. Wallace, J.I. Hanoka, in: Proceedings of the 26th IEEE Photovoltaic Specialists Conference, Anaheim, 1997, p. 95.
[45] A.M. Gabor, D.L. Hutton, J.I. Hanoka, in: Proceedings of the 16th European PV Solar Energy Conference, Glasgow, 2000, p. 2083.
[46] H. Lange, I.A. Schwirtlich, J. Crystal Growth 104 (1990) 108.
[47] I. Steinbach, H.-U. Höfs, in: Proceedings of the 26th IEEE Photovoltaic Specialists Conference, Anaheim, 1997, p. 91.
[48] C. Zechner, G. Hahn, W. Jooss, M. Wibral, B. Bitnar, S. Keller, M. Spiegel, P. Fath, G. Willeke, E. Bucher, in: Proceedings of the 26th IEEE Photovoltaic Specialists Conference, Anaheim, 1997, p. 243.
[49] A. Eyer, N. Schillinger, S. Schelb, A. Räuber, J. Crystal Growth 82 (1987) 151.
[50] A. Eyer, N. Schillinger, I. Reis, A. Räuber, J. Crystal Growth 104 (1990) 119.
[51] A. Goetzberger, A. Räuber, in: Proceedings of the ISES Solar World Congress, Kobe, Pergamon, Oxford, 1989.
[52] W. Zimmermann, S. Bau, A. Eyer, F. Haas, D. Osswald, in: Proceedings of the 16th European PV Solar Energy Conference, Glasgow, 2000, p. 1144.
[53] A. Rohatgi, D.L. Meier, T.W. O'Keeffe, P. Rai-Choudhury, in: Proceedings of the 18th IEEE Photovoltaic Specialists Conference, Las Vegas, 1985, p. 50.
[54] S. Narasimha, G. Crotty, T. Krygowski, A. Rohatgi, D.L. Meier, in: Proceedings of the 26th IEEE Photovoltaic Specialists Conference, Anaheim, 1997, p. 235.
[55] M. Wolf, in: Proceedings of the 14th IEEE Photovoltaic Specialists Conference, San Diego, 1980, p. 674.
[56] M. Spitzer, J. Shewchun, E.S. Vera, J.J. Loferski, in: Proceedings of the 14th IEEE Photovoltaic Specialists Conference, San Diego, 1980, p. 375.
[57] A. Goetzberger, in; Proceedings of the 15th IEEE Photovoltaic Specialists Conference, Kissimmee, 1981, p. 867.
[58] A. Goetzberger, J. Knobloch, B. Voss, Tech. Dig. Int. PVSEC-1 (1984) 517.
[59] C. Hebling, A. Eyer, F.R. Faller, A. Hurrle, R. Lüdemann, S. Reber, W. Wettling, Festkörperprobleme/Adv. Solid State Phys. 38 (1998) 607.
[60] J.H. Werner, S. Kolodinski, H.J. Queisser, Phys. Rev. Lett. 72 (1994) 3851.
[61] R.B. Bergmann, Appl. Phys. A 69 (1999) 187–194.
[62] S. Reber, W. Wettling, Appl. Phys. A 69 (1999) 215–220.
[63] J. Poortmans, A. Diet, A. Raeuber, in: Proceedings of the 16th European PV Solar Energy Conference, Glasgow, 2000, p. 1076.
[64] K.R. Catchpole, M.J. McCann, A.W. Blakers, K.J. Weber, in: Proceedings of the 16th European PV Solar Energy Conference, Glasgow, 2000, p. 1165.
[65] J.R. Davis, et al., IEEE Trans. Electron Devices ED-27 (4) (1980) 677.
[66] J. Isenberg, S. Reber, J. Aschaber, W. Warta, in: Proceedings of the 16th European PV Solar Energy Conference, Glasgow, 2000, p. 1463.
[67] S. Reber, Electrical confinement for the crystalline silicon thin-film solar cell on foreign substrate, Dissertation, University of Mainz, 2000.
[68] J.A.M. van Roosmalen, C.J.J. Took, R.C. Huiberts, R.J.G. Beenen, J.P.P. Huijsmans, W.C. Sinke, in: Proceedings of the 25th IEEE-PVSC, 1996, p. 657.
[69] I. Silier, M. Konuma, A. Gutjahr, E. Bauser, in: Proceedings of the 25th IEEE-PVSC, 1996, p. 681.
[70] R. Lüdemann, S. Schaefer, C. Schüle, C. Hebling, in: Proceedings of the 26th IEEE-PVSC, Anaheim, 1997, p. 159.

[71] K. Yamamoto, M. Yoshimi, T. Suzuki, Y. Okamoto, Y. Tawada, A. Nakajima, in: Proceedings of the 26 IEEE-PVSC, Anaheim, 1997, p. 575.
[72] M.A. Green, J. Zhao, G. Zheng, in: Proceedings of the 14th European Photovoltaic Solar Energy Conference, Barcelona, 1997, p. 2324.
[73] J. Zhao, A. Wang, G.F. Zheng, S.R. Wenham, M.A. Green, in: Proceedings of the 13th IEEE Photovoltaic Specialists Conference, Nice, 1995, p. 1642.
[74] F.R. Faller, A. Hurrle, N. Schillinger, MRS Spring Meeting, San Francisco, 1998.
[75] S. Reber, G. Stollwerck, D. Osswald, T. Kieliba, C. Häßler, in: Proceedings of the 16th European PV Solar Energy Conference, Glasgow, 2000, p. 1136.
[76] C. Hebling, S.W. Glunz, J.O. Schumacher, J. Knobloch, in: Proceedings of the 14th European Photovoltaic Solar Energy Conference, Barcelona, 1997, p. 2318.
[77] C. Hebling, Die kristalline Silicium-Dünnschichtsolarzelle auf isolierenden Substraten, Dissertation, University of Konstanz, 1998.
[78] A. Takami, S. Arimoto, H. Morikawa, S. Hamamoto, T. Ishihara, H. Kumabe, T. Murotani, in: Proceedings of the 12th EC-PVSEC, 1994, p. 59.
[79] T. Mishima, S. Itoh, G. Matuda, M. Yamamoto, K. Yamamoto, H. Kiyama, in: Proceedings of the Technical Digest of the 9th PVSEC, Miyazaki, 1996, p. 243.
[80] A.M. Barnett, Prog. Photovolt. 5 (1997) 317.
[81] G.F. Zheng, Z. Shi, R. Bergmann, X. Dai, S. Robinson, A. Wang, J. Kurianski, M.A. Green, Solar Energy Mater. Solar Cells 32 (1994) 129.
[82] R. Brendel, in: Proceedings of the 14th European PVSEC, 1997, p. 1354.
[83] K.R. Catchpole, K.J. Weber, A.B. Sproul, A.W. Blakers, in: Proceedings of the 2nd World Conference on Photovoltaic Energy Conversion, 1998, p. 1336.
[84] S. Hamamoto, H. Morikawa, H. Naomoto, Y. Kawama, A. Takami, S. Arimoto, T. Ishihara, K. Namba, in: Proceedings of the 14th European PVSEC, Barcelona, 1997, p. 2328.
[85] H. Tayanaka, K. Yamaguchi, T. Matsushita, in: Proceedings of the 2nd World Conference on PV Solar Energy Conversion, 1998, p. 1272.
[86] T.J. Rinke, R.B. Bergmann, J.H. Werner, in: Proceedings of the 16th European PV Solar Energy Conference, Glasgow, 2000, p. 1128.
[87] R. Brendel, in: Proceedings of the 2nd World Conference on Photovoltaic Solar Energy Conversion, Vienna, 1998, p. 1242.
[88] K.J. Weber, K. Catchpole, M. Stocks, A.W. Blakers, in: Proceedings of the 26th IEEE Photovoltaic Specialists Conference, Anaheim, 1997, p. 107.
[89] R. Auer, J. Zettner, J. Krinke, G. Polliski, T. Hierl, R. Hezel, M. Schulz, H.-P. Strunk, F. Koch, D. Nikl, H.V. Campe, in: Proceedings of the 26th IEEE Photovoltaic Specialists Conference, Anaheim, 1997, p. 739.
[90] J.S. Rand, J.E. Cotter, C.J. Thomas, A.E. Ingram, Y.B. Bai, T.R. Ruffins, A.M. Barnett, in: Proceedings of the 1st World Conference on Photovoltaics, Hawaii, 1994, p. 1262.
[91] G. Balhorn, K.J. Weber, S. Armand, M.J. Stocks, A.W. Blakers, Solar Energy Mater. Solar Cells 52 (1998) 61.
[92] A.W. Blakers, K.J. Weber, M.F. Stuckings, S. Armand, G. Matlakowski, A.J. Carr, M.J. Stocks, A. Cuevas, T. Brammer, Prog. Photovolt. 3 (1995) 193.
[93] K. Ishii, H. Nikishikawa, T. Takahashi, Y. Hayashi, Jpn. J. Appl. Phys. 32 (1993) 770.
[94] R. Shimokawa, T. Takahashi, H. Takato, A. Ozaki, Y. Takano, in: Proceedings of the 16th European PV Solar Energy Conference, Glasgow, 2000, p. 1565.
[95] F.R. Faller, N. Schillinger, A. Hurrle, C. Schetter, in: Proceedings of the 14th European Photovoltaic Solar Energy Conference, Barcelona, 1997, p. 784.
[96] T. Kieliba, S. Reber, in: Proceedings of the 16th European PV Solar Energy Conference, Glasgow, 2000, p. 1455.
[97] C. Hebling, S. Reber, K. Schmidt, R. Lüdemann, F. Lutz, in: Proceedings of the 26th IEEE Photovoltaic Specialists Conference, Anaheim, 1997, p. 623.
[98] T. Uematsu, M. Ida, K. Hane, S. Kokunai, T. Saitoh, IEEE Trans. Electron Devices ED-37 (2) (1990) 344.
[99] T. Vermeulen, F. Duerinckx, K. De Clerq, J. Szlufcik, J. Poortmans, P. Laermans, M. Caymax, J. Nijs, R. Mertens, in: Proceedings of the 26th IEEE Photovoltaic Specialists Conference, Anaheim, 1997, p. 267.
[100] T. Vermeulen, O. Evrard, W. Laureys, J. Poortmans, M. Caymax, J. Nijs, R. Mertens, C. Vinckier, H.U. Höfs, in: Proceedings of the 13th European Photovoltaic Solar Energy Conference, Nice, 1995, p. 1501.
[101] A. Takami, S. Arimoto, H. Morikawa, S. Hamamoto, T. Ishihara, H. Kumabe, T. Murotani, Jpn. J. Appl. Phys. 33 (1994) 1396.
[102] H. Morikawa, Y. Nishimoto, H. Naomoto, Y. Kawama, A. Takami, S. Arimoto, T. Ishihara, K. Namba, Solar Energy Mater. Solar Cells 53 (1998) 23.
[103] H. Naomoto, S. Hamamoto, A. Takami, S. Arimoto, T. Ishihara, Solar Energy Mater. Solar Cells 48 (1997) 261.
[104] J.H. Werner, J.K. Arch, R. Brendel, G. Langguth, M. Konuma, E. Bauser, G. Wagner, B. Steiner, W. Appel, in: Proceedings of the 12th European Photovoltaic Solar Energy Conference, Amerdam, 1994, p. 1823.
[105] R. Brendel, M. Hirsch, M. Stemmer, U. Rau, J.H. Werner, Appl. Phys. Lett. 66 (10) (1995) 1261.

[106] T.F. Ciszek, J. Crystal Growth 66 (1984) 655.
[107] T. Baba, M. Shima, T. Matsuyama, S. Tsuge, K. Wakisaka, S. Tsuda, in: Proceedings of the 13th European Photovoltaic Solar Energy Conference, Nice, 1995, p. 1708.
[108] F. Tamura, Y. Okayasu, K. Kumagai, in: in: Proceedings of the Technical Digest on International PVSEC-7, 1993, p. 237.
[109] A. Shah, J. Meier, P. Torres, U. Kroll, D. Fischer, N. Beck, N. Wyrsch, H. Keppner, in: Proceedings of the 26th IEEE Photovoltaic Specialists Conference, Anaheim, 1997, p. 569.
[110] Z. Shi Zheng, S.R. Wenham, Prog. Photovolt. 2 (1994) 153.
[111] Z. Shi, S.R. Wenham, Prog. Photovolt. 2 (1994) 153.
[112] K. Feldrapp, D. Scholten, S. Oelting, H. Nagel, M. Steinhof, R. Auer, R. Brendel, in: Proceedings of the 16th European PV Solar Energy Conference, Glasgow, 2000, p. 1703.
[113] R.C. Chittick, J.H. Alexander, H.F. Sterling, J. Electrochem. Soc. 116 (1969) 77.
[114] W.E. Spear, P.G. LeComber, J. Non-Cryst. Solids 810 (1972) 727.
[115] D. Carlson, C. Wronski, Appl. Phys. Lett. 28 (1976) 671.
[116] H. Fritzsche, Mater. Res. Soc. Symp. Proc. 609 (2000).
[117] D.L. Staebler, C.R. Wronski, Appl. Phys. Lett. 31 (1977) 292.
[118] T. Suntola, in: Proceedings of the 11th EC Photovoltaic Solar Energy Conference, Montreux, 1992, p. 977.
[119] Y. Tawada, H. Yamagishi, in: Proceedings of the Technical Digest on International PVSEC-11, Sapporo, 1999, Tokyo University of Agriculture and Technology, Tokyo, p. 53.
[120] S. Guha, Prog. Photovolt.: Res. Appl. 8 (2000) 141.
[121] S. Guha, S. Yang, S. Glattfelder, Proceedings of the 2nd World Conference on Photovoltaic Solar Energy Conversion, Vienna, 1998, p. 3609.
[122] J. Meier, P. Torres, R. Platz, S. Dubail, U. Kroll, J. Anna, N. Selvan, Pellaton, Vaucher, Ch. Hof, D. Fischer, H. Keppner, A. Shah, J. Koehler, Mater. Res. Symp. Proc. 420 (1996) 3.
[123] J. Meier, H. Keppner, S. Dubail, U. Kroll, P. Torres, P. Pernet, Y. Ziegler, J.A. Anna, N. Selvan, J. Cuperus, D. Fischer, A. Shah, in: Proceedings of the MRS Symposium, Spring Meeting, San Francisco, vol. 507, 1998, pp. 139–144.
[124] C. Koch, M. Ito, V. Svrcek, M.B. Schubert, J.H. Werner, Mater. Res. Soc. Symp. Proc. 609 (2002) A15.6.1–A15.6.6.
[125] H. Sakata, K. Kawamoto, M. Taguchi, T. Baba, S. Tsuge, K. Uchihashi, N. Nakamura, S. Kiyam, in: Proceedings of the 28th IEEE Photovoltaic Specialists Conference, Anchorage, Alaska, USA, 2000, p. 7.
[126] S. Wagner, J.L. Shay, P.P. Migliorato, H.M. Kasper, Appl. Phys. Lett. 25 (1974) 434.
[127] L.L. Kazmerski, F.R. White, G.K. Morgan, Appl. Phys. Lett. 46 (1976) 268.
[128] K.C. Mitchell, E.J. Ermer, D. Pier, in: Proceedings of the Conference Record on 20th IEEE Photovoltaic Specialists Conference, Las Vegas, IEEE Press, Piscataway, 1988, p. 1384.
[129] T. Haalboom, T. Gödecke, F. Ernst, M. Rühle, R. Herberholz, H.-W. Schock, C. Beilharz, K.W. Benz, Inst. Phys. Conf. Ser. 152E (1997) 249–252.
[130] S.B. Zhang, S.H. Wei, A. Zunger, H. Katayama-Yoshida, Phys. Rev. B 57 (1998) 9642.
[131] D. Schmid, M. Ruckh, F. Grunwald, H.W. Schock, J. Appl. Phys. 73 (1993) 2902.
[132] R. Herberholz, U. Rau, H.-W. Schock, T. Halboom, T. Gödecke, F. Ernst, C. Beilharz, K.W. Benz, D. Cahen, Eur. Phys. J. Appl. Phys. 6 (1999) 131–139.
[133] U. Rau, H.W. Schock, Appl. Phys. A 69 (1999) 131.
[134] H. Kushiya, M. Tachiyuki, Y. Nagoya, A. Fujimaki, B. Sang, D. Okimura, M. Satoh, O. Yamase, in: Proceedings of the Technical Digest on International PVSEC-11, Sapporo 1999, Tokyo University of Agriculture and Technology, Tokyo, p. 637.
[135] F. Karg, in: Proceedings of the Technical Digest on 11th Photovoltaic Solar Cell Engineering Conference, Sapporo, 1999, p. 627.
[136] C. Eberspacher, K. Pauls, J. Serra, Unisun, Camarillo, CA, Mater. Res. Soc. Symp. Proc. 668 (2001) H2.5.1.
[137] F. Dimroth, O.V. Sulima, A.W. Bett, Comp. Semicond. Mag. 6 (6) (2000) 1.
[138] S. Wiedemann, R.G. Wendt, J.S. Britt, in: Proceedings of the NCPV Photovoltaics Program Review Meeting, 1998 (AIP CP 462), p. 17.
[139] B. Dimmler, H.W. Schock, Prog. Photovolt.: Res. Appl. 4 (1996) 425–433.
[140] M. Powalla, B. Dimmler, in: Proceedings of the 16th European Photovoltaic Solar Energy Conference, Glasgow, 2000.
[141] T. Nakada, T. Mise, T. Kume, A. Kunioka, in: Proceedings of the 2nd World Conference on Photovoltaic Solar Energy Conversion, Vienna, European Commission, 1998, p. 413.
[142] M.A. Contreras, B. Egaas, K. Ramanathan, J. Hiltner, A. Swartzlander, F. Hason, R. Noufi, Prog. Photovolt.: Res. Appl. 7 (1999) 311.
[143] H.W. Schock, R. Noufi, Prog. Photovolt.: Res. Appl. 8 (2000) 151–160.
[144] J. Kessler, M. Bodegard, J. Hedström, L. Stolt, in: Proceedings of the 16th European Photovoltaic Solar Energy Conference, Glasgow, 2000, p. 2057.
[145] C.R. Leidholm, G.A. Norsworthy, R. Roe, A. Halani, B.M. Basol, V.K. Kapur, in: M. Al-Jassim, J.P. Thornton, J.M. Gee (Eds.), Proceedings of the AIP Conference, vol. 462, 1999, p. 103.

[146] C. Fredric, C. Eberspaecher, K. Pauls, J. Serra, J. Zhu, M. Al-Jassim, J.P. Thornton, J.M. Gee (Eds.), in: Proceedings of the AIP Conference, vol. 462, 1998, p. 158.
[147] R. Herberholz, V. Nadenau, U. Rühle, C. Köble, H.W. Schock, B. Dimmler, Solar Energy Mater. Solar Cells 49 (1997) 227.
[148] V. Nadenau, D. Hariskos, H.W. Schock, in: Proceedings of the 14th European Photovoltaic Solar Energy Conference, Barcelona, H.S. Stephens & Associates, Bedford, 1997, p. 1250.
[149] K. Siemer, J. Klaer, I. Luck, J. Bruns, R. Klenk, D. Bräunig, in: Proceedings of the Technical Digest on International PVSEC-11, Sapporo, 1999, Tokyo University of Agriculture and Technology, Tokyo, p. 623.
[150] H.W. Schock, R. Noufi, Prog. Photovolt.: Res. Appl. 8 (2000) 151–160.
[151] D.A. Cusano, Solid State Electron. 6 (1963) 217.
[152] A.L. Fahrenbruch, R.H. Bube, Academic Press, New York, 1983.
[153] Ken Zweibel, Harnessing Solar Power —The Photovoltaic Challenge, 1990.
[154] R.H. Bube, Photovoltaic Materials, Imperial College Press, London, 1998.
[155] Y. Tyan, E.A. Perez-Albuerne, in: Proceedings of the 16th IEEE Photovoltaic Specialists Conference, San Diego, CA, USA, 1982, p. 794.
[156] C. Ferekides, J. Britt, Y. Ma, L. Killian, in: Proceedings of the 23rd IEEE Photovoltaic Specialists Conference, Louisville, USA, 1993, p. 389.
[157] P.V. Meyers, S.P. Albright, Prog. Photovolt.: Res. Appl. 8 (2000) 161.
[158] L.M. Woods, D.H. Levi, V. Kaydanov, G.Y. Robinson, R.K. Ahrenkiel, in: Proceedings of the NCPV Photovoltaics Program Review Meeting, 1998 (AIP CP 462), p. 499.
[159] D.W. Cunningham, K. Davies, L. Grammond, J. Healy, E. Mopas, N. O'Connor, M. Rubcich, W. Sadeghi, D. Skinner, T. Trumbly, in: Proceedings of the 16th European Photovoltaic Solar Energy Conference, Glasgow, 2000, p. 281.
[160] A.W. Bett, F. Dimroth, M. Meusel, U. Schubert, R. Adelhelm, in: Proceedings of the 16th European PV Solar Energy Conference, Glasgow, 2000, p. 951.
[161] C. Stalder, J. Augustynski, J. Electrochem. Soc. 126 (1997) 2007.
[162] B. O'Regan, M. Grätzel, Nature 252 (1991) 737.
[163] M. Grätzel, Nature (London) 403 (2000) 363.
[164] J. Ferber, R. Stangl, J. Luther, Solar Energy Mater. Solar Cells 53 (1998) 29.
[165] A. Hinsch, J.M. Kroon, M. Späth, J.A.M. van Roosmalen, N.J. Bakker, P. Sommeling, N. Burg, R. van der Kinderman, R. Kern, J. Ferber, C. Schill, M. Schubert, A. Meyer, T. Meyer, I. Uhlendorf, J. Holzbock, R. Niepmann, in: Proceedings of the 16th International Photovoltaic Solar Energy Conference, Glasgow, 2000, p. 32.
[166] R.H. Bossert, C.J.J. Tool, J.A.M. van Roosmalen, C.H.M. Wentink, M.J.M. de Vaan, Report of November 2000.
[167] U. Bach, Nature 395 (1998) 583; ICSM 2000.
[168] Toshiba, in: Proceedings of the 16th International Photovoltaic Solar Energy Conference, Glasgow, 2000.
[169] D. Meissner, Photon Int. 2 (1999) 34.
[170] D. Meissner, in: Proceedings of the ICSM 2000.
[171] N.S. Sariciftci, L. Smilowitz, A.J. Heeger, F. Wudl, Science 258 (1992) 1474.
[172] J. Rostalski, D. Meissner, Solar Energy Mater. 61 (2000) 87.
[173] O. Inganäs, et al., in: L. Chen et al. (Eds.), Proceedings of the ICSM 2000, Adv. Mater. 12 (2000) 1367.
[174] J. Schön, Ch. Kloc, B. Batlogg, in: Proceedings of the 16th International Photovoltaic Solar Energy Conference, Glasgow, 2000, p. 43.
[175] P.T. Landsberg, H. Nussbaumer, G. Willeke, J. Appl. Phys. 74 (2) (1993).
[176] S. Kolodinski, J.H. Werner, T. Wittchen, H.J. Queisser, Appl. Phys. Lett. 63 (1993) 1451.
[177] J.H. Werner, B. Winter, M. Wolf, S. Kolodinski, R. Brendel, M. Hirsch, H.J. Queisser, J. Wollweber, W. Schröder, in: Proceedings of the 13th European PV Solar Energy Conference, Nice, France, 1995, p. 111.
[178] R.T. Ross, A.J. Nozic, J. Appl. Phys. 53 (1982) 3818.
[179] P. Würfel, Solar Energy. Mater. Solar Cells 46 (1997) 43.
[180] A. Luque, A. Martí, Phys. Rev. Lett. 78 (1997) 5014.
[181] A. Luque, A. Martí, L. Cuadra in: Proceedings of the 16th European PV Solar Energy Conference, Glasgow, 2000, p. 59.
[182] A. Martí, L. Cuadra, A. Luque, in: Proceedings of the 16th European PV Solar Energy Conference, Glasgow, 2000, p. 15.
[183] G. Yu, J. Gao, J.C. Hummelen, F. Wudl, A.J. Heeger, Science 270 (1995) 1789.s.